Applying Dependable and Secure Protection With Quadrilateral Distance Elements

Kanchanrao Dase, Armando Guzmán, Steven Chase, and Brian Smyth
Schweitzer Engineering Laboratories, Inc.

Presented at the
77th Annual Conference for Protective Relay Engineers at Texas A&M
College Station, Texas
March 26–28, 2024

Original release October 2022

Applying Dependable and Secure Protection With Quadrilateral Distance Elements

Kanchanrao Dase, Armando Guzmán, Steven Chase, and Brian Smyth, *Schweitzer Engineering Laboratories, Inc.*

***Abstract*—This paper analyzes factors affecting the performance of current polarized reactance elements and provides guidelines to ensure the security of Zone 1 quadrilateral distance elements. Network nonhomogeneity, instrument transformer errors, line charging currents, line transpositions, zero-sequence mutual coupling, and unbalanced operating conditions affect the performance of current polarized reactance elements. This paper evaluates each of these factors in detail and determines an overall tilt angle for the Zone 1 reactance element. Using this tilt angle for a given right resistance blinder setting ensures security of Zone 1 quadrilateral distance elements, assuming the correct operation of directional and fault-type identification logics. This paper demonstrates how lowering the right resistance blinder setting value reduces the necessary tilt for the reactance element characteristic. This demonstration will assist relay engineers to determine settings based on expected values of fault resistances over the length of the protected zone. This paper analyzes reactance elements polarized with negative-sequence, zero-sequence, and loop currents.**

I. Introduction

Distance relays are typically used to protect power lines. They provide primary protection for in-line faults –without communications channels– and backup protection for out-of-section faults. In 1928, Warrington designed an electromechanical reactance relay that included two reactance elements supervised by an admittance (mho) element [1]. Fig. 1 shows the operating characteristic of this relay in the impedance plane. This relay has three operating zones for line protection:

- Zone 1 (reactance), the reach of which is set to less than the line impedance (Z_{1L}) and provides instantaneous protection for in-line faults.
- Zone 2 (reactance), the reach of which is set beyond the line impedance and provides primary protection for in-line faults that are not seen in Zone 1 and backup protection for external faults.
- Zone 3 (mho), the reach of which is set beyond the Zone 2 reach, supervises Zones 1 and 2, and provides backup protection for external faults.

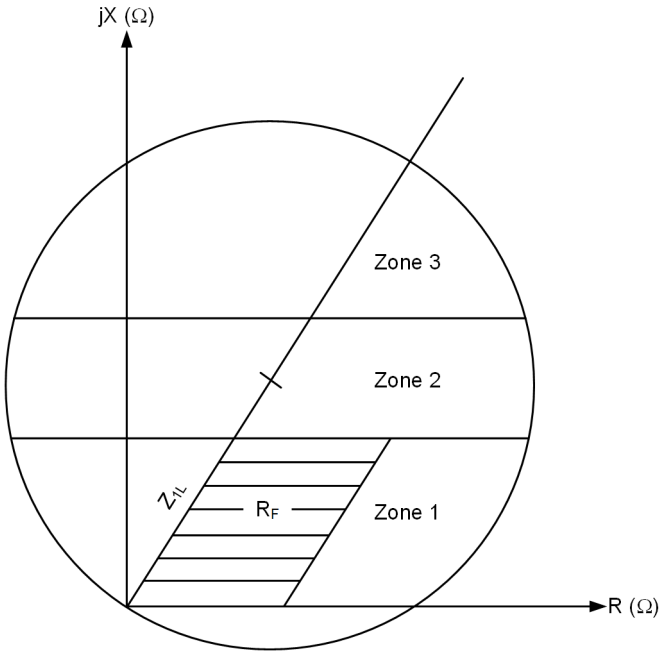

Fig. 1. Operating characteristic of the reactance relay designed by Warrington.

Warrington assumed the error in the reactance component (X_{ER}) introduced by the fault resistance (R_F) was negligible. Therefore, he used horizontal lines to represent the R_F values for different fault locations, as shown in Fig. 1. There are many fault conditions in which X_{ER} may be significant. For example, a resistive single-line-to-ground (SLG) fault at the end of the line with the remote terminal open may have a significant X_{ER}, as illustrated in Fig. 2. The apparent impedance (Z_{APP}) in this example is given by (1), where X_{ER} is $\mathrm{Im}[R_F / (1 + k_0)]$. In general, k_0 is not a real number; therefore, $\mathrm{Im}[R_F / (1 + k_0)]$ is not zero. In Fig. 2, the angle of k_0 is negative.

$$Z_{APP} = Z_{1L} + \frac{R_F}{1 + k_0} \tag{1}$$

where:

$k_0 = \dfrac{Z_{0L} - Z_{1L}}{3 \bullet Z_{1L}}$ is the zero-sequence compensation factor.

Z_{1L} is the positive-sequence line impedance.

Z_{0L} is the zero-sequence line impedance.

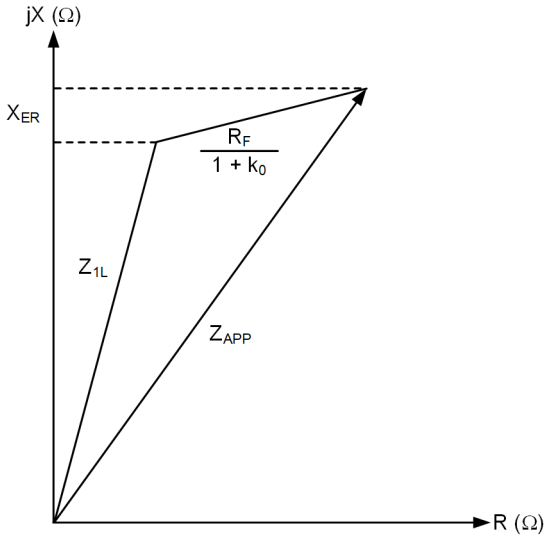

Fig. 2. Apparent impedance Z_{APP} for an SLG fault at the end of the line with the remote terminal open and fault resistance R_F.

Line loading also causes a significant effect on X_{ER} [2]. Fig. 3 illustrates this behavior for an A-phase-to-ground (AG) fault at the end of the line with outgoing line load. Note the clockwise tilt of $[I_F \bullet R_F / I_L]$ with respect to the horizontal representation in Fig. 1. In many cases, R_F can have high values depending on tower footing resistance or in the absence of shield wires, or because of faults caused by flashover to a tree or brush fires [3]. In Fig. 3, I_F is the total fault current at the fault location and I_L is the loop current.

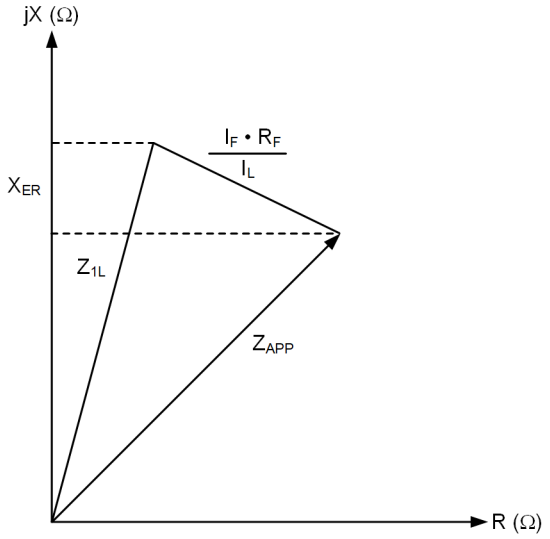

Fig. 3. Apparent impedance Z_{APP} for an AG fault at the end of the line with outgoing load and fault resistance R_F.

Warrington's relay uses phase current as the polarizing quantity for the reactance elements (depicted by horizontal lines limiting Zones 1 and 2 in Fig. 1) of the ground distance elements [4]. The operating characteristic of reactance elements that use phase current polarization tilts clockwise or counterclockwise for different loading conditions, which results in element over- or underreach [5][1].

Let us demonstrate how the polarizing quantity affects the reach of the reactance element by considering a fault at a distance *m* per unit (pu) from the relay, as shown in Fig. 4.

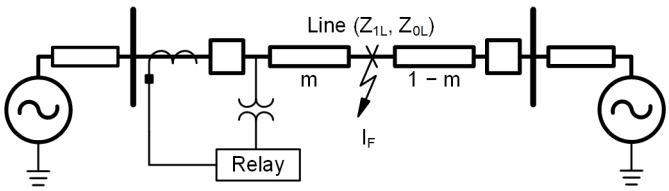

Fig. 4. Two-source power system with a fault at a distance *m* per unit from the relay.

The voltage V_L at the relay location can be expressed as shown in (2).

$$V_L = m \bullet Z_{IL} \bullet I_L + I_F \bullet R_F \tag{2}$$

Dividing both the sides of (2) by the polarizing current I_P, and taking imaginary parts, we get (3).

$$\mathrm{Im}\left[\frac{V_L}{I_P}\right] = \mathrm{Im}\left[\frac{m \bullet Z_{1L} \bullet I_L}{I_P}\right] + \mathrm{Im}\left[\frac{I_F \bullet R_F}{I_P}\right] \tag{3}$$

Writing $\mathrm{Im}[I_F \bullet R_F / I_P]$ from (3) in polar form results in (4).

$$\mathrm{Im}\left[\frac{V_L}{I_P}\right] = \mathrm{Im}\left[\frac{m \bullet Z_{1L} \bullet I_L}{I_P}\right] + \left[\frac{I_F \bullet R_F}{I_P}\right] \sin\left(\angle I_F - \angle I_P\right) \tag{4}$$

In (4), $\mathrm{Im}[V_L / I_P]$ is the relay calculated impedance based on the choice of I_P. When I_P is set to I_L, the term $\mathrm{Im}[V_L / I_P]$ is referred as the reactance component of the apparent impedance. If the polarizing quantity angle ($\angle I_P$) equals the fault current angle ($\angle I_F$), $\sin(\angle I_F - \angle I_P)$ is zero and the relay calculated impedance ($\mathrm{Im}[V_L / I_P]$), using (4), corresponds to the actual reach impedance ($\mathrm{Im}[m \bullet Z_{1L} \bullet I_L / I_P]$), resulting in no reach errors. When $\angle I_P$ leads $\angle I_F$, $\sin(\angle I_F - \angle I_P)$ is negative and the relay calculated impedance ($\mathrm{Im}[V_L / I_P]$), using (4), is smaller than the corresponding actual reach impedance ($\mathrm{Im}[m \bullet Z_{1L} \bullet I_L / I_P]$), causing overreach. When $\angle I_P$ lags $\angle I_F$, $\sin(\angle IF - \angle IP)$ is positive and the relay calculated impedance ($\mathrm{Im}[V_L / I_P]$), using (4), is greater than the corresponding actual reach impedance ($\mathrm{Im}[m \bullet Z_{1L} \bullet I_L / I_P]$), causing underreach. In summary, the polarizing quantity leading the fault current results in overreach, whereas the polarizing quantity lagging the fault current causes underreach. In case of Warrington's reactance element (Fig. 1), the use of phase current as a polarizing quantity does not follow the fault current angle. In fact, the phase current can either lead or lag the fault current depending on the loading conditions, resulting in the corresponding over- or underreach of the phase current polarized reactance element.

With advancements in electronic circuit technology, the quadrilateral (also known as "polygonal") characteristic was introduced by some manufacturers. In 1970, the polygonal characteristic was introduced in a three-phase static protective relay [6]. In 1971, E. Zurowski introduced the quadrilateral

[1] This paper refers to the rotation of a vector by a negative angle as clockwise tilt and by a positive angle rotation as counterclockwise tilt.

characteristic in a static protective relay, as described in [7]. In these characteristics, the resistive R and reactive X reaches are set independently. Fig. 5 shows the quadrilateral characteristic with the corresponding resistive and reactance settings, R_{SET} and X_{SET}.

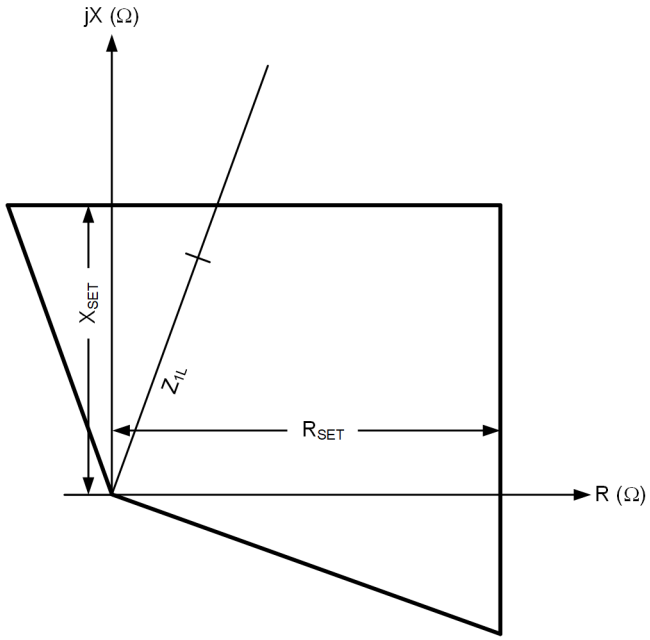

Fig. 5. Quadrilateral characteristic in a static protective relay introduced by E. Zurowski.

The reactance element of this quadrilateral characteristic uses loop current as polarization. The impedance plots in Fig. 6 illustrate under- and overreaching conditions of this quadrilateral characteristic for different R_F values and loading conditions [2] [8]. The angles mentioned in Fig. 6 are of the local voltage source behind the relay in reference to the remote voltage source angle.

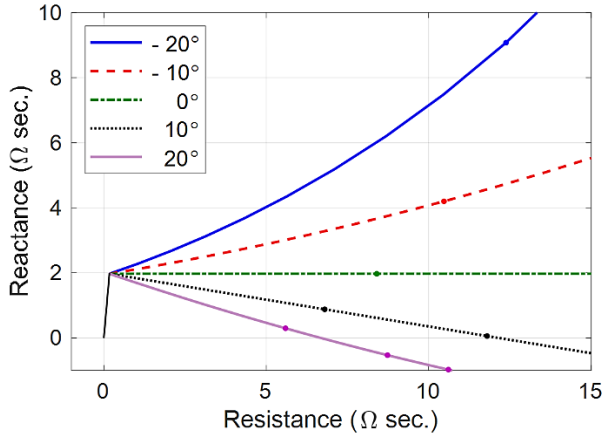

Fig. 6. Apparent fault impedance for varying fault resistance for incoming (solid blue and red dash lines) and outgoing (black dash and solid magenta lines) loads.

A relay with the loop polarized characteristic, as shown in Fig. 5, underreaches for incoming load when the polarizing quantity (loop current) lags the fault current and overreaches for outgoing load when the polarizing quantity (loop current) leads the fault current. Typically, the loop polarized reactance elements need to have the reactance characteristic tilted clockwise, e.g., –15 degrees [9], to avoid overreach. However, in many cases, this tilt angle for the loop polarized reactance element characteristic may not be sufficient to compensate for heavy outgoing loading conditions.

Reference [5] describes a quadrilateral characteristic with a reactance element that uses the residual current (three times the zero-sequence current, $3 \bullet I_0$) as the polarizing quantity. Another choice for polarization is the negative-sequence current ($3 \bullet I_2$). These polarizing quantities have the same angle as the fault current angle for homogenous systems, irrespective of load flow, theoretically resulting in no under- or overreach. For nonhomogenous networks, these polarizing quantities need correction.

This paper analyzes the effects of network nonhomogeneity, instrument transformer errors, line charging currents, line transpositions, zero-sequence mutual coupling, and unbalanced operating conditions on the reactance element characteristics that use negative-sequence, zero-sequence, and loop current polarization. The paper focuses on providing guidance on how to set the Zone 1 distance element to prevent element overreach.

II. Factors Affecting the Security of Zone 1 Quadrilateral Distance Elements

Table I summarizes the factors affecting the security of the Zone 1 quadrilateral distance elements. These factors are typically compensated by reducing the Zone 1 reach and/or tilting the Zone 1 reactance characteristic in a clockwise direction. An alternative to clockwise tilting of the reactance characteristic is to reduce the right resistance blinder reach setting. The security impact of Factors 1–7 and 9–10 in Table I on Zone 1 distance elements and the corresponding compensation through modification of the Zone 1 reach are explained in [10]. The effect of coupling capacitor voltage transformer (CCVT) transients (Factor 5 in Table I) may also be compensated through built-in relay security logic or by intentionally delaying the Zone 1 element. The Zone 1 overreach concerns, due to zero-sequence mutual coupling (Factor 9 in Table I), may also be addressed through the modification of the zero-sequence compensation factor [11] [12].

This paper focuses on addressing Factors 3, 6, and 8–14 listed in Table I by modifying the tilt of the reactance element, except in the case of Factor 11 (current transformer [CT] saturation), which is compensated through the reactance element reach. For reference, Table II summarizes typical polarizing quantities for different fault types.

Sections III, V, VII, and X use the simulation results based on the power system shown in Fig. 7. Note that the impedance values used here are in primary ohms.

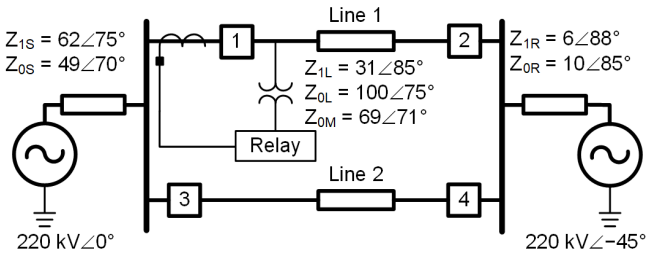

Fig. 7. Power system used in Sections III, V, VII, and X.

TABLE I
FACTORS AFFECTING SECURITY OF ZONE 1 QUADRILATERAL DISTANCE ELEMENTS

Factors Affecting Zone 1 Security	Compensation Modifying	
	Zone 1 Reach	Tilt of Reactance Element
1. Line parameters (positive- and zero-sequence impedance).	✓	
2. Infeed and outfeed for tapped or multiterminal lines [13].	✓	
3. Relay steady-state errors.	✓ (Magnitude errors)	✓ (Angle errors)
4. Transient overreach.	✓	
5. CCVT transients (may also be compensated through the security logic in the relay or by intentionally delaying Zone 1).	✓	
6. Voltage transformer (VT) steady-state magnitude and angle errors.	✓ (Magnitude errors)	✓ (Angle errors)
7. Voltage induction in secondary cables and ground potential rise.	✓	
8. Network nonhomogeneity and line loading.		✓
9. Zero-sequence mutual coupling (may also be compensated through modifying zero-sequence compensation factor).	✓	✓
10. CT steady-state magnitude and angle errors.	✓ (Magnitude errors)	✓ (Angle errors)
11. CT saturation.	✓	
12. Line charging current.		✓
13. Untransposed line.		✓
14. Unbalanced operating conditions (may also be addressed through the security logic in the relay).		✓
15. Subharmonic-frequency transient in series-compensated lines [14].	✓	

TABLE II
POLARIZING QUANTITIES FOR VARIOUS FAULT TYPES

Fault Type	Polarizing Quantity		
	Negative-Sequence Current ($3 \bullet I_2$)	Zero-Sequence Current ($3 \bullet I_0$)	Loop Current (I_L)
AG	$3 \bullet I_{A2}$	$3 \bullet I_0$	$I_A + k_0 \bullet I_G$
BG	$3 \bullet I_{B2}$	$3 \bullet I_0$	$Ib + k_0 \bullet I_G$
CG	$3 \bullet I_{C2}$	$3 \bullet I_0$	$I_C + k_0 \bullet I_G$
AB or ABG	$3 \bullet I_{A2} - 3 \bullet I_{B2}$	–	$I_A - I_B$
BC or BCG	$3 \bullet I_{B2} - 3 \bullet I_{C2}$	–	$I_B - I_C$
CA or CAG	$3 \bullet I_{C2} - 3 \bullet I_{A2}$	–	$I_C - I_A$
ABC	–	–	$I_A - I_B$, $I_B - I_C$, $I_C - I_A$

III. CALCULATING THE NONHOMOGENOUS NETWORK AND LOAD CORRECTION ANGLE FOR CORRESPONDING POLARIZING QUANTITIES

A. Calculating the Nonhomogenous Network Correction Angle for Negative-Sequence Current Polarization

In general, the nonhomogenous network correction angle for the negative-sequence network (θ_{2_NW}) is defined as the angle difference between the negative-sequence fault current and the relay measured negative-sequence current. Some relays may refer this correction angle as TANG [9].

For the system shown in Fig. 8 and the corresponding negative-sequence network in Fig. 9, (5) provides the negative-sequence current nonhomogenous network correction angle.

$$\theta_{2\_NW} = \arg\left(\frac{I_{2F}}{I_L}\right) \tag{5}$$

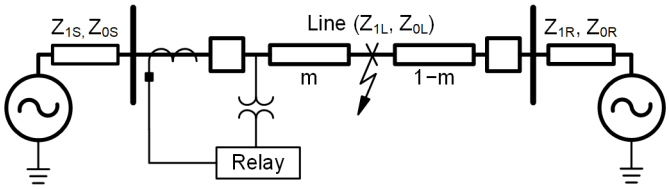

Fig. 8. Two-source power system with a single-line configuration.

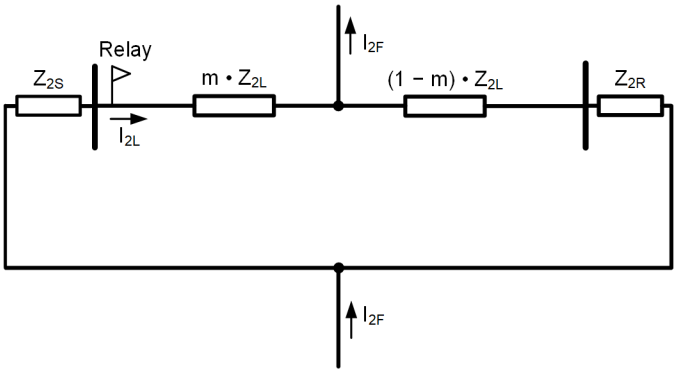

Fig. 9. Negative-sequence network for the system shown in Fig. 8.

Equation (5) is usually defined in terms of negative-sequence network parameters. For the negative-sequence network in Fig. 9, (5) can be expressed by (6).

$$\theta_{2\_NW\_SL} = \arg\left[\frac{Z_{2S} + Z_{2L} + Z_{2R}}{(1-m)\bullet Z_{2L} + Z_{2R}}\right] \quad (6)$$

For Zone 1 elements, the nonhomogenous network correction angle is typically calculated for a fault at the Zone 1 reach [9]. However, to achieve an adequate negative-sequence nonhomogenous network angle, consider faults at the Zone 1 reach and at the remote end of the line ($m = 1$) with a weak source behind the relay and a strong source at the remote end. Note that (6) is applicable for single-line configurations, not for parallel lines originating from and terminating on a common bus, as shown in Fig. 10. For such a parallel line configuration with both lines in service, (7) is used to determine the negative-sequence current nonhomogenous network correction angle. Refer to Appendix A for the derivation of (7).

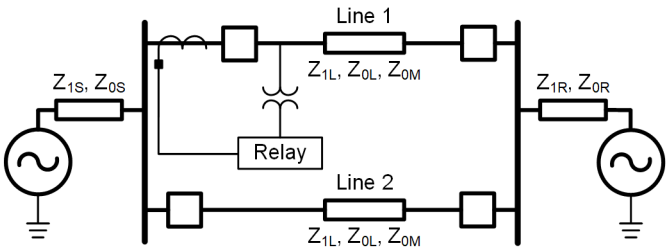

Fig. 10. Two-source power system with parallel lines originating from and terminating on a common bus.

$$\theta_{2\_NW\_PL} = -\arg\left[\frac{(1-m)\bullet(Z_{2S} + Z_{2L} + Z_R) + Z_{2R}}{2\bullet\left(Z_{2S} + \frac{Z_{2L}}{2} + Z_{2R}\right)}\right] \quad (7)$$

In parallel line configurations, one of the lines can be out of service. Therefore, consider the minimum of the nonhomogenous network correction angles from (6) and (7). If there is the possibility of a scenario in which the lines originate from different buses but terminate on a common bus, as shown in Fig. 11, consider the protected line (Line 1) as a single line of a two-source power system, similar to the one shown in Fig. 8, and use (6) to calculate the single-line nonhomogenous network correction angle. Note that in this case, the negative-sequence source impedance at the remote end is not only Z_{1R}, but also involves Z_{1L2} and Z_{1S2}.

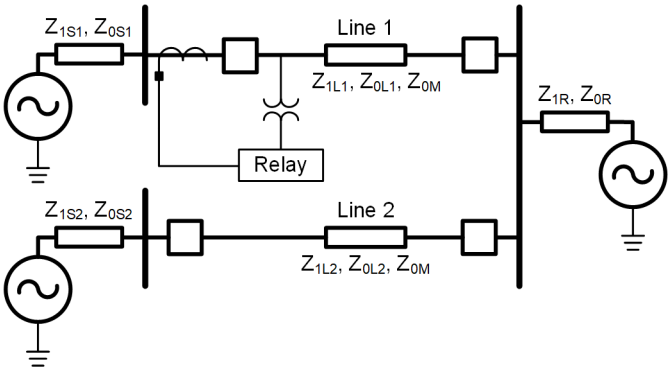

Fig. 11. Two-source power system with lines originating from different buses but terminating on a common bus.

Fig. 11 shows the change in the negative-sequence nonhomogenous network correction angle for faults at different locations over the length of the line for the system shown in Fig. 7. The plots in Fig. 12 are for the relay located at Breaker 1 when either of the following operating conditions occur:

- Line 1 and Line 2 are in service.
- Line 1 is in service, and Line 2 is out of service (Breakers 3 and 4 are open).

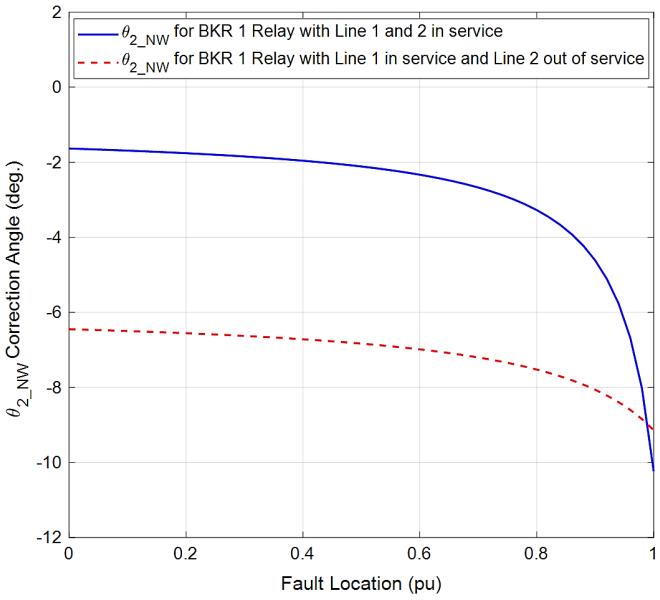

Fig. 12. Negative-sequence nonhomogenous network correction angle (θ_{2_NW}) for faults at different locations over the length of the line for the system shown in Fig. 7 for the relay located at Breaker 1.

TABLE III
NEGATIVE-SEQUENCE NONHOMOGENOUS NETWORK CORRECTION ANGLE (Θ_{2_NW}) FOR SYSTEM IN FIG. 7 FOR THE RELAYS LOCATED AT BREAKER 1

θ_{2_NW}	m = 0.8 (pu)	m = 1 (pu)
$\theta_{2\_NW\_SL}$ (Lines 1 and 2 in service)	–7°	–9°
$\theta_{2\_NW\_SL}$ (Line 1 in service and Line 2 out of service)	–3°	–10°

Because Zone 1 is an underreaching element, choose the minimum of the nonhomogenous network angles calculated at $m = 0.8$ pu (Zone 1 reach) and $m = 1$ pu for the single and parallel line configurations using (6) and (7), respectively. Therefore, from Table III, the negative-sequence nonhomogenous network correction angle for the relay at Breaker 1 is –10 degrees. To determine the correction angle for the relay at Breaker 2, use the same approach described in this section; however, consider a weak source behind the relay at Breaker 2 and a strong source at the other end.

B. Calculating the Nonhomogenous Network Correction Angle for Zero-Sequence Current Polarization

Calculate the zero-sequence nonhomogenous network correction angle for a single-line configuration using (8). To achieve an adequate correction angle, consider faults at the Zone 1 reach and the remote end of the line ($m = 1$) with a weak source behind the relay and a strong source at the remote end of the line.

$$\theta_{0\_NW\_SL} = \arg\left(\frac{I_{0F}}{I_{0L}}\right) = \arg\left[\frac{Z_{0S} + Z_{0L} + Z_{0R}}{(1-m)\bullet Z_{0L} + Z_{0R}}\right] \quad (8)$$

For mutually coupled line configurations, the zero-sequence line impedance becomes a function of the zero-sequence mutual impedance and the zero-sequence current of the mutually coupled lines. Fig. 13 shows the change in the zero-sequence impedance of the line due to the current in the parallel circuit for a fault at a distance m per unit from the relay. In this case, the mutually coupled lines originate and terminate at the same buses.

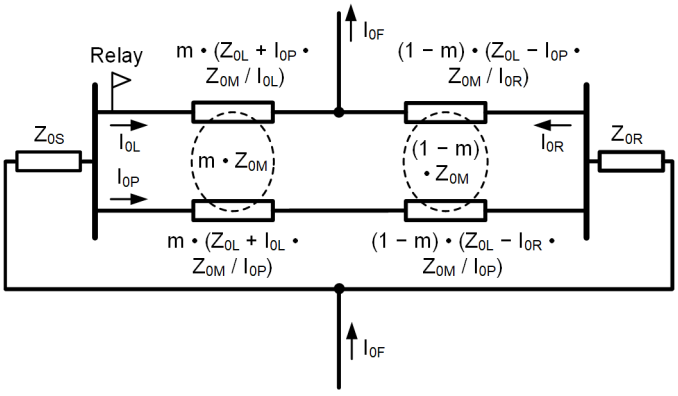

Fig. 13. Zero-sequence network for a fault at distance m from the relay in a configuration with two mutually coupled lines originating and terminating at the same buses.

Representing mutual coupling in the zero-sequence network can be complicated for multicircuit lines, especially for the ones that do not run along the entire length of the protected line. Therefore, short-circuit simulation tools are convenient to calculate the zero-sequence nonhomogenous network correction angle, especially at the Zone 1 reach. For line-end faults, the zero-sequence network complexity is significantly reduced. Note the reduced complexity in Fig. 14, which is the same as Fig. 13; however, in this case, there is a fault at the remote end of the line.

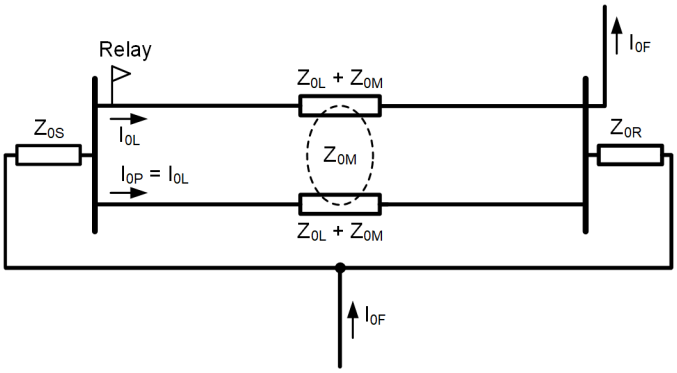

Fig. 14. Zero-sequence network for a fault at the remote end of the line in a configuration with two mutually coupled lines originating and terminating at the same buses.

Equations (9) and (10) give the zero-sequence nonhomogenous network correction angle for faults at the remote end of the protected line, which is mutually coupled with n other lines. Equation (9) assumes all the n mutually coupled lines originate and terminate at the same buses, where $k = 1$ indicates the protected line. Use (10) for mutually coupled lines that do not originate or terminate at a common bus or are partly in parallel with the protected line. As previously explained, merge the parallel line impedances with the appropriate source impedances for mutually coupled lines with only one common bus. If short-circuit simulation tools are not available, use (9) or (10) to get the zero-sequence nonhomogenous network correction angle for faults at $m = 1$. Note that (10) requires the values of the zero-sequence currents of the adjacent lines for faults at the remote end of the protected line, along with the corresponding zero-sequence mutual impedance values.

$$\theta_{0\_NW\_PL}\big|_{m=1} = \arg\left(\frac{n\bullet\left(Z_{0S} + \frac{Z_{0L}}{n} + Z_{0R}\right) + \sum_{k=2}^{n} Z_{0M_{1,k}}}{Z_{0R}}\right) \quad (9)$$

$$\theta_{0\_NW\_PL'}\big|_{m=1} = \arg\left(\frac{Z_{0S} + Z_{0L} + Z_{0R} + \sum_{k=2}^{n}\left(\frac{I_{0P_k}}{I_{0L}}\right) Z_{0M_{1,k}}}{Z_{0R}}\right) \quad (10)$$

Fig. 15 shows the change in the zero-sequence nonhomogenous network correction angle for different fault locations over the length of the line for the system shown in Fig. 7. The plots in Fig. 15 are for the relay located at Breaker 1 when either of the following conditions occur:

- Line 1 and Line 2 are in service.
- Line 1 is in service, and Line 2 is out of service (Breakers 3 and 4 are open).

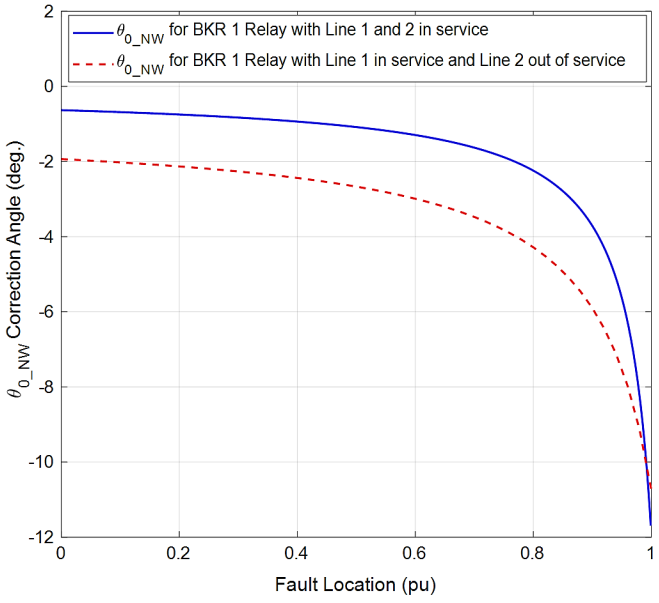

Fig. 15. Zero-sequence nonhomogenous network correction angle (θ_{0_NW}) for different fault locations over the length of the line for the system shown in Fig. 7, for the relay located at Breaker 1.

TABLE IV
ZERO-SEQUENCE NONHOMOGENOUS NETWORK CORRECTION ANGLE (Θ_{0_NW}) FOR THE SYSTEM IN FIG. 7, FOR THE RELAY LOCATED AT BREAKER 1

θ_{0_NW}	m = 0.8 (pu)	m = 1 (pu)
$\theta_{0\_NW\_SL}$	–4°	–11°
$\theta_{0\_NW\_PL}$	–2°	–12°

Because Zone 1 is an underreaching element, choose the minimum of the nonhomogenous network correction angles, calculated at m = 0.8 pu (Zone 1 reach) and m = 1 pu for single and mutually coupled lines originating and terminating at the same buses. Therefore, from Table IV, we can conclude that the zero-sequence nonhomogenous network correction angle for the relay at Breaker 1 is –12 degrees. To determine the correction factor for the relay at Breaker 2, use the same approach described previously in this section; however, consider a weak source behind the relay at Breaker 2 and a strong source at the other end.

C. *Calculating the Load Correction Angle for Loop Current Polarization*

As summarized in Table II, the loop currents for different fault types are functions of the phase currents. For resistive faults, the faulted phase current measured by the relay is the superposition of the fault and load currents. Therefore, loop currents cannot accurately provide the fault current angle; therefore, a correction is needed to ensure security of the reactance element [2]. Equation (11), in general, defines the loop current correction angle for faults at the remote end of the protected line. Equation (11) gives the minimum angle difference between the fault current and the corresponding fault-type loop current for different fault resistances (in primary ohms) at the remote end of the line. Short-circuit calculation tools are convenient to solve (11). To achieve an adequate correction angle, consider maximum outgoing power flow from the protective relay point of view for all possible source impedances.

$$\theta_{L\_LOAD}\Big|_{m=1} = \min\left[\arg\left(\frac{I_F}{I_L}\right) \quad \forall \quad 1 \le R_F < 100\right] \tag{11}$$

Fig. 16 shows the angle difference between the fault current and the loop current for SLG faults at the remote end of the line with varying fault resistances. The plots in Fig. 16 are for the system shown in Fig. 7, for the relay located at Breaker 1, when either of the following conditions occur:

- Line 1 and Line 2 are in service.
- Line 1 is in service, and Line 2 is out of service (Breakers 3 and 4 are open).

Because the faults are simulated at the remote end of the protected line, when the mutually coupled lines in service originate and terminate at the same buses, we use the modified zero-sequence compensation factor in (11) [11].

$$k_{0L\_PL} = \left(\frac{Z_{0L} + Z_{0M} - Z_{1L}}{3 \bullet Z_{1L}}\right) \tag{12}$$

From Fig. 16, we can conclude that the minimum angle difference between the fault current and the corresponding relay loop current at Breaker 1 is –34 degrees. Therefore, from (11), θ_{L_LOAD} is the loop current correction angle for the relay at Breaker 1 for SLG faults. To determine an adequate loop current correction angle for multiphase fault loops, use the same approach described in this section; however, consider multiphase faults at the remote end of the line. To determine an adequate loop current correction angle for the relay at Breaker 2, use the same approach described in this section; however, consider reversing the power flow in the system, as shown in Fig. 7, such that the relay at Breaker 2 measures the maximum outgoing power when faults are simulated at the remote end of the line.

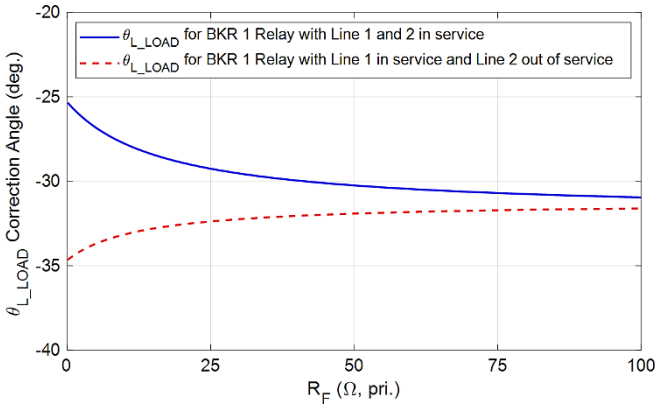

Fig. 16. Angle difference between the fault current and the corresponding loop current (θ_{L_LOAD}) measured by the relay at Breaker 1 in Fig. 7 for SLG faults at the remote end of the line.

IV. Calculating the Negative- and Zero-Sequence Nonhomogenous Network Correction Angle for Lines With Low-Impedance Angles

This section explains calculating the nonhomogenous network correction angles for lines with an impedance angle less than 70 degrees. Low line impedance angles are particularly common in underground cables [15]. Fig. 17 shows an example of a subtransmission underground cable of 15 miles that connects the two sources of the power system. Note that the impedance values used in this example are in primary ohms. To calculate an adequate nonhomogenous network correction angle, consider a weak source behind the relay and a strong source at the remote end. The following example evaluates only the use of (6) for calculating the negative-sequence nonhomogeneous correction angle for lines with low-impedance angles. A similar analysis can be extended by using (8) for calculating the zero-sequence nonhomogenous correction angle for lines with low-impedance angles.

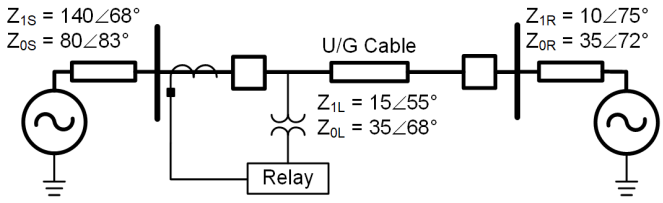

Fig. 17. Two-source subtransmission power system with an underground cable connecting the two sources.

Using (6) and based on the selected values of source impedances in Fig. 17, the negative-sequence nonhomogenous network correction angle for a fault at the remote bus (m = 1 pu) is –8 degrees. Consider using this clockwise tilt for the negative-sequence polarized Zone 1 reactance element.

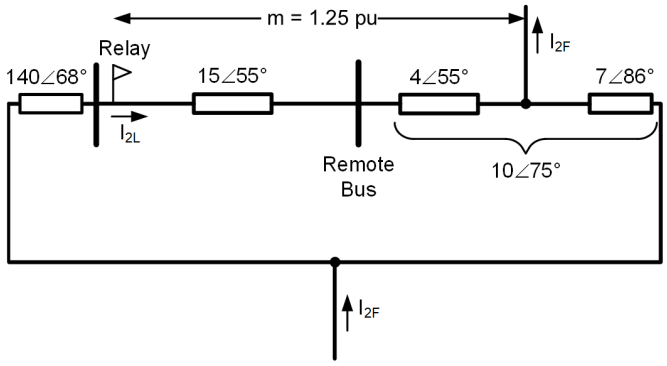

Fig. 18. Negative-sequence network for the system in Fig. 17 for an unbalanced fault beyond the remote bus.

Fig. 18 shows the negative-sequence network for an unbalanced fault beyond the remote bus (m = 1.25 pu). Notice that the remote impedance is modeled as a combination of impedances, such that the total impedance beyond the remote bus is still the same as that shown in Fig. 17. Using (6), the negative-sequence correction angle for a fault at m = 1.25 pu equals –9 degrees, which is lower than the correction angle of –8 degrees considered for the Zone 1 reactance element. Because of this angle difference, the Zone 1 quadrilateral distance element may overreach for resistive faults beyond the remote bus (see Fig. 19). Fig. 19 shows the reactance element characteristics at Zone 1 reach (Z_{1R}) and m = 1.25 pu, with correction angles of –8 degrees and –19 degrees, respectively.

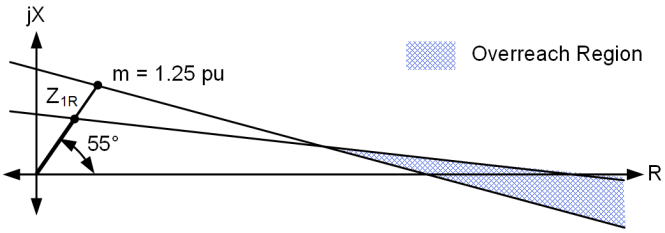

Fig. 19. Operating characteristics of reactance elements at Zone 1 reach (Z_{1R}) and m = 1.25 pu for an unbalanced fault at m = 1.25 pu.

In Fig. 19, if the right resistance blinder is set in such a way that its characteristic falls on the left of the intersection of the two reactance characteristics, then the Zone 1 element is secure; otherwise, it is not. However, determining that setting of the right resistance blinder is not easy. Alternatively, the simplest way is to apply a nonhomogenous network correction angle, from (13), to the negative-sequence current polarized Zone 1 reactance element. The acronym "SL_LZA_NW," used in (13) and (14), stands for a single-line configuration with a low impedance angle in a nonhomogenous network.

$$\theta_{2\_SL\_LZA\_NW} = \arg\left(Z_{2S} + Z_{2L}\right) - 88° \qquad (13)$$

Equation (13) is a simplified form of (6), with m = 1 and assuming that the strongest theoretical possible remote impedance (e.g., $|Z_{2R}|$ = 1 mΩ) has a very high impedance angle (e.g., $\angle Z_{2R}$ = 88 degrees). These assumptions result in a higher clockwise tilt angle value compared to the one obtained from (6); thus, prevent overreach issues like the one illustrated in Fig. 19. Therefore, for applications with lines having low negative-sequence impedance angle (less than 70 degrees)

consider using (13), instead of (6), to calculate the negative-sequence nonhomogenous correction angle. Similarly, consider using (14), instead of (8), to calculate the zero-sequence nonhomogenous correction angle for lines with low zero-sequence impedance angle (less than 70 degrees).

$$\theta_{0\_SL\_LZA\_NW} = \arg\left(Z_{0S} + Z_{0L}\right) - 88° \quad (14)$$

Using (13) and (14), the negative- and zero-sequence nonhomogenous network correction angles for the relay protecting the underground cable in Fig. 17 equal –21 degrees and –10 degrees, respectively.

V. Calculating the Faulted Phase Voltage and Polarizing Quantity Angle Errors Because of VT and CT Steady-State Angle Errors

The errors of the primary and relay instrument transformers may cause underreach or overreach of the Zone 1 distance elements [16] [17]. To secure the Zone 1 elements, the instrument transformer magnitude errors for line-end metallic faults ($R_F = 0$) are typically compensated by reducing the Zone 1 reach. Equation (15) gives an expression for the error in the reactance element reach, $\Psi_{m\_IT\_ANG}$ (in pu), in terms of the angle errors of the faulted phase voltage (θ_{V_ERR}) and the polarizing current of the reactance element (θ_{IPOL_ERR}). The acronym "IT_ANG" in $\Psi_{m\_IT\_ANG}$ stands for instrument transformer angle error. Refer to Appendix B for the derivation of (15). In this equation, the VT and CT magnitude errors are ignored because these errors are assumed to be compensated by the Zone 1 reach setting. The polarizing current angle, in primary amperes, is assumed to be the same as the fault current angle. Therefore, θ_{IPOL_ERR} has only CT angle errors. Negative values of $\Psi_{m\_IT\_ANG}$ indicate overreach, whereas positive values indicate underreach. Note that (15) is an approximate expression and therefore may have numerical errors. However, (15) is still valuable for illustrating the effect of instrument transformer angle errors on reach estimation.

$$\Psi_{m\_IT\_ANG} \approx \cot\left(\theta_V - \theta_{I_F}\right) \bullet \left(\theta_{V\_ERR} - \theta_{I_{POL\_ERR}}\right) \quad (15)$$

where:

$(\theta_V - \theta_{IF})$ is the angle difference between the faulted phase voltage at the relay location and the total fault current.

θ_{V_ERR} is the error in the faulted phase voltage angle because of the primary and relay VTs.

θ_{IPOL_ERR} is the error in the polarizing current angle because of the primary and relay CTs.

In (15), the angle $(\theta_V - \theta_{IF})$ is expected to decrease as the fault resistance increases, resulting in increasing overreach or underreach depending on the angle error $(\theta_{V\_ERR} - \theta_{IPOL\_ERR})$. Fig. 20 illustrates instances of reactance element overreach for different values of $(\theta_{V\_ERR} - \theta_{IPOL\_ERR})$. On the abscissa, the angle $(\theta_V - \theta_{IF})$ is reduced from 90 degrees to 10 degrees, indicating an increase in the fault resistance, while the ordinate shows $\Psi_{m\_IT\_ANG}$ for different values of $(\theta_{V\_ERR} - \theta_{IPOL\_ERR})$. Note that for high fault resistances (low values of $[\theta_V - \theta_{IF}]$), even a low value of $(\theta_{V\_ERR} - \theta_{IPOL\_ERR})$ causes a significant error in the reach of the reactance element. To avoid reactance element overreach because of instrument transformer angle errors, the reactance element characteristic needs to be tilted clockwise by an angle of $(\theta_{V\_ERR} - \theta_{IPOL\_ERR})$. The following example illustrates how to compensate reactance element overreach because of instrument transformer angle errors.

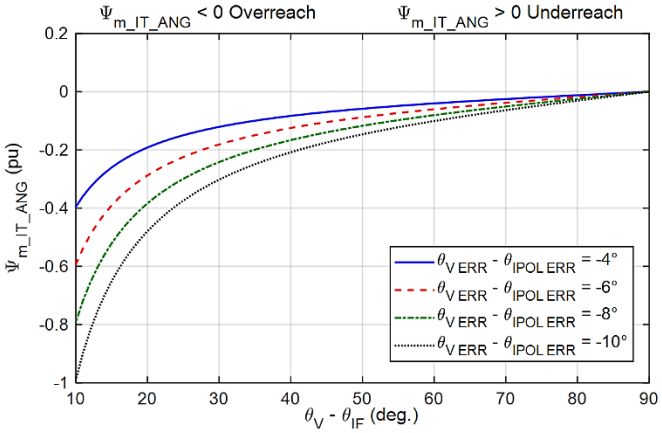

Fig. 20. Effect of increasing the fault resistance (reducing $[\theta_V - \theta_{IF}]$) on reactance element overreach for different instrument transformers angle errors.

For the example system shown in Fig. 7, consider an AG metallic fault ($R_F = 0$) at the end of the line for a heavy loading condition and a weak source behind the relay. Table V shows the phase currents for this fault with and without CT angle errors and the corresponding polarizing quantities derived from the phase currents. We assumed a steady-state CT angle error of ±2 degrees in each of the phase currents. Note that an angle error of ±2 degrees in the phase currents may translate to a higher angle error in the polarizing quantity (θ_{IPOL_ERR}). Taking the values of (θ_{IPOL_ERR}) from Table V and assuming –2 degrees of angle error in the faulted phase voltage (θ_{V_ERR}), the total angle error $(\theta_{V\_ERR} - \theta_{IPOL\_ERR})$ affecting the reach of the negative-sequence, zero-sequence, and loop current polarized reactance elements equals 0, –7, and –6 degrees, respectively.

Table V
Current Phasors and Polarizing Quantity Angle Errors for a Line-End Metallic AG Fault in the Fig. 7 System

	Ideal Phasors	Phasors With Angle Errors	θ_{IPOL_ERR}
Phase Currents	$I_A = 720\angle -49°$	$I_A' = 720\angle -47°$	–
	$I_B = 574\angle -112°$	$I_B' = 574\angle -110°$	–
	$I_C = 590\angle 126°$	$I_C' = 590\angle 124°$	–
Corresponding Polarizing Quantities	$3 \bullet I_2 = 642\angle -101°$	$3 \bullet I_2' = 632\angle -103°$	–2°
	$3 \bullet I_0 = 605\angle -99°$	$3 \bullet I_0' = 578\angle -94°$	5°
	$I_L = 1006\angle -73°$	$I_L' = 1004\angle -69°$	4°

In Table V, because the phase current angle errors (±2 degrees) were introduced randomly, we cannot rely on the

minimum values of the polarizing quantity angle errors. Therefore, for the example system of Fig. 7 and assuming ±2 degrees of steady-state angle error in the CTs and PTs, consider tilting the negative-sequence, zero-sequence, or loop polarized reactance element characteristics clockwise by 7 degrees (maximum of $|\theta_{V\_ERR} - \theta_{IPOL\_ERR}|$) to avoid reactance element overreach because of instrument transformer angle errors.

In summary, to avoid reactance element overreach because of instrument transformer angle errors, determine (θ_{IPOL_ERR}) for different possible values of the CT angle error in the phase currents and tilt the reactance element characteristic clockwise by the maximum value of ($|\theta_{V\_ERR} - \theta_{IPOL\_ERR}|$). Calculate the phase currents for a line-end metallic fault ($R_F = 0$), with heavy line loading and the weakest source behind the relay.

VI. Effect of CT Saturation on the Reactance Element Reach

Ideally, CTs are not expected to saturate for faults at the remote end of the line. However, saturation may occur for line-end faults in short lines with strong systems. When a CT saturates, the resulting current phasor has a reduced magnitude and a leading phase angle shift [18]. Typically, the reduction in magnitude of the faulted phase current results in underreach of the reactance element. However, the leading phase angle shift of the faulted phase current may result in a leading or lagging phase angle shift of the polarizing quantity, causing the element to overreach or underreach for resistive faults. Equation (16) shows an approximate expression to determine the error in the reactance element reach, $\Psi_{m\_CT\_SAT}$ (in pu), caused by CT saturation, assuming no error in the faulted phase voltage magnitude and angle. Refer to Appendix B for the derivation of (16). Negative values of $\Psi_{m\_CT\_SAT}$ indicate overreach, whereas positive values indicate underreach.

$$\Psi_{m\_CT\_SAT} \approx I_{L\_MAG\_ERR}\left[1-\cot\left(\theta_V-\theta_{I_F}\right)\bullet\left(\theta_{I_{POL\_ERR}}\right)\right]-1 \quad (16)$$

where:

$I_{L\_MAG\_ERR} = \left|\frac{I_{L\_UNSAT}}{I_{L\_SAT}}\right|$ is the magnitude of the ratio of the unsaturated faulted loop current (I_{L_UNSAT}) to the saturated faulted loop current (I_{L_SAT}).

($\theta_V - \theta_{IF}$) is the angle difference between the faulted phase voltage at the relay location and the total fault current.

(θ_{IPOL_ERR}) is the error in the polarizing current angle because of CT saturation.

Equation (16) is helpful when the user knows ($I_{L\_MAG\_ERR}$) and (θ_{IPOL_ERR}) for different values of ($\theta_V - \theta_{IF}$) for line-end faults that cause local CT saturation. Note that (16) may not hold true for severe CT saturation, resulting in $|\theta_{IPOL\_ERR}|$ being greater than 20 degrees because the angle error assumptions made in deriving (16) are no longer valid. However, the parameters in (16) affecting the error in the reactance element reach, $\Psi_{m\_CT\_SAT}$, still apply. Based on (16), consider the following points when using short-circuit programs to evaluate the Zone 1 quadrilateral element security for line-end faults that cause local CT saturation:

- Fault resistance affects ($\theta_V - \theta_{IF}$). As the fault resistance increases, ($\theta_V - \theta_{IF}$) decreases, and the leading angle (positive value) of θ_{IPOL_ERR} because of CT saturation may cause an increase in $\Psi_{m\_CT\_SAT}$. Metallic faults will most likely cause underreach.
- Loading conditions affect ($I_{L\_MAG\_ERR}$) and (θ_{IPOL_ERR}).
- Several factors affect CT saturation, e.g., saturation voltage of the CT, CT burden, fault current, remanence, CT ratio, CT winding resistance [19].

If the CT saturation results in overreach of the reactance element, the Zone 1 reach may have to be reduced appropriately to ensure its security.

VII. Calculating the Polarizing Quantity Angle Error Because of Line Charging Current

This section demonstrates the effect of line charging current on the negative-sequence, zero-sequence, and loop polarizing quantities. When the negative- and zero-sequence networks have line and source impedance angles close to 90 degrees (i.e., greater than 85 degrees), the shunt capacitance currents of negative- and zero-sequence networks are either in phase or out of phase with the negative- and zero-sequence relay currents, respectively [20]. Therefore, there is negligible impact on the angle error between the relay current and the total fault current when compared to the same network without shunt capacitances. Typically, the relay negative- and zero-sequence voltages are smaller than the positive-sequence voltage. This makes the shunt charging currents that are directly proportional to the magnitude of the voltage less significant in the zero- and negative-sequence networks.

Consider the example system of Fig. 7, with a metallic AG fault ($R_F = 0$) at the end of the line with the weakest source behind the relay. To avoid the effect of mutual coupling, the parallel line is kept out of service. Table VI shows the angles of the negative-sequence, zero-sequence, and loop polarizing quantities with respect to the total fault current with and without considering the line shunt capacitances. We used Electromagnetic Transients Program (EMTP) software to model these conditions.

TABLE VI
NEGATIVE-SEQUENCE, ZERO-SEQUENCE, AND LOOP POLARIZED CURRENT ANGLES FOR LINE-END FAULT WITH AND WITHOUT LINE SHUNT CAPACITANCE

Polarizing Quantity Angle With Respect to Total Fault Current Angle	With Line Capacitance (1)	Without Line Capacitance (2)	(1) – (2)
$\angle 3 \bullet I_2 - \angle I_F$	8.6°	9.1°	–0.5°
$\angle 3 \bullet I_0 - \angle I_F$	10.4°	10.8°	–0.4°
$\angle I_L - \angle I_F$	36.8°	35.8°	1°

Table VI shows that the angles of the zero- and negative-sequence currents for the line model with shunt capacitance are smaller than the ones for the line without shunt capacitance. The smaller angles of these polarizing currents result in underreach of the corresponding reactance element. Therefore, no compensation is needed for the zero- and negative-sequence polarized reactance element for the example system in Fig. 7. However, the loop current for the line model with shunt capacitance is greater than the one without line shunt capacitance by one degree. This greater angle must be compensated for to avoid overreach by tilting the loop polarized reactance element characteristic clockwise by one degree.

VIII. Calculating the Polarizing Quantity Angle Error in Lines Without Transpositions

This section explains how to estimate the polarizing quantity angle error in untransposed line applications. The EMTP simulation results, shown in this section, are based on a horizontal transmission line configuration (see Fig. 21). We simulated SLG faults at the remote end of this untransposed line in a perfectly homogenous system. Therefore, the angle difference between the negative- or zero-sequence current and the fault current is the error in the respective polarizing quantity solely due to the lack of transpositions. Had we considered an ideally transposed line in a perfectly homogenous system, the angle difference between the negative- or zero-sequence current and the fault current would have been zero.

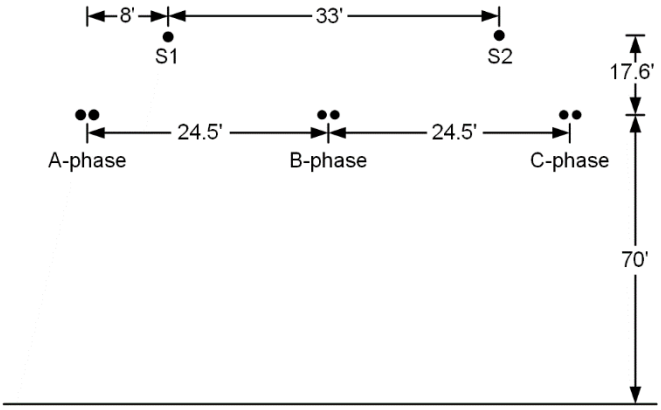

Fig. 21. Typical 345 kV transmission line tower configuration.

To calculate the loop current angle errors in untransposed line applications, use EMTP software and find the angle difference between the loop current and the fault current for an ideally transposed line; then, subtract it from the angle difference between the loop current and the fault current for the untransposed line.

Table VII summarizes the angle errors for negative-sequence, zero-sequence, and loop polarized currents for SLG faults at the remote end of the line for outgoing and incoming loading conditions. A positive angle error means that the corresponding polarizing quantity leads the fault current phasor, which causes reactance element overreach. A negative angle error in the polarizing quantity indicates reactance element underreach.

Table VII
Error in the Negative-Sequence, Zero-Sequence, and Loop Polarized Current Angles Because of Untransposed (UT) Line

Fault	Angle Error, in Degrees, for		
	I_{2_UT}	I_{0_UT}	I_{L_UT}
AG (outgoing power)	1.1	–0.1	0.5
BG (outgoing power)	2.3	–0.8	0.1
CG (outgoing power)	–3.5	0	–0.6
AG (incoming power)	2.3	–0.5	0.2
BG (incoming power)	–2.3	–0.2	–0.2
CG (incoming power)	–0.5	–0.5	0.0

Based on the results summarized in Table VII, tilt the negative-sequence reactance element characteristic by at least 2.3 degrees in the clockwise direction to avoid the overreach caused by the untransposed line. The characteristic of the zero-sequence current polarized reactance element needs no tilt, and the loop current polarized reactance element characteristic requires only 0.5 degrees of tilt in the clockwise direction. Note that the results summarized in Table VII are for SLG faults. Therefore, the angle errors are suitable only for the ground reactance elements. Use a similar approach to determine the angle errors for the phase reactance elements, simulating multiphase faults.

IX. Calculating the Polarizing Quantity Angle Error Because of Unbalanced Operating Conditions

This paper defines unbalanced operating conditions as unbalanced loading, open phase caused by a broken conductor or breaker operation, a pole open in a parallel line, pole discrepancy while clearing multiphase faults, breaker failure, or asymmetrical series capacitor switching. In general, transmission and distribution networks with single- and three-pole tripping protection schemes are subjected to unbalanced operating conditions. Occurrence of a resistive fault under such conditions corrupts the polarizing current of the reactance element, resulting in element underreach or overreach. The following example demonstrates reactance element overreach conditions because of a resistive fault in an unbalanced network.

In the Fig. 22 example system, consider a resistive AG fault at the remote end of the protected line without (Fig. 22 (a)) and with (Fig. 22 (b)) an open-phase condition. No magnetic mutual coupling is considered between the parallel lines and the impedance values are in primary ohms. For the AG fault and the system conditions shown in Fig. 22, ($3 \bullet I_{2\_FLT}$), ($3 \bullet I_{0\_FLT}$), and (I_{L_FLT}) are the relay measured negative-sequence, zero-sequence, and loop current phasors, in primary amperes. Whereas, ($3 \bullet I_{2\_UB}$), ($3 \bullet I_{0\_UB}$), and (I_{L_UB}) are the relay measured primary negative-sequence, zero-sequence, and loop current phasors because of the unbalanced operating condition (Phase A open in a parallel line) prior to the occurrence of the fault (Fig. 22 (b)). The value, I_{FLT}, is the total fault current, in primary amperes, and the reference for the other phasors listed in Table VIII and Table IX. Because the system is homogenous,

no tilt is considered for the zero- and negative-sequence current polarized reactance elements. However, to account for outgoing loading, a tilt of –7 degrees is assumed for the loop polarized reactance element.

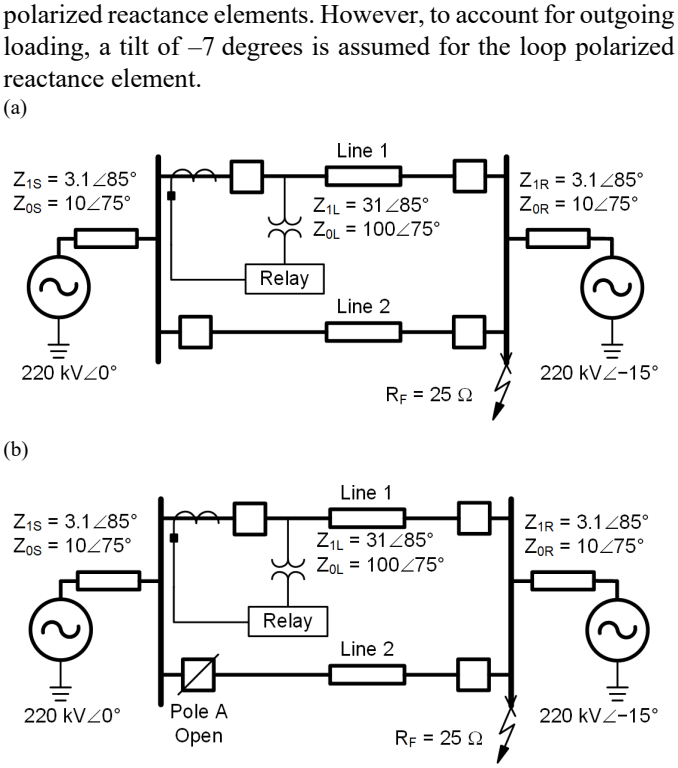

Fig. 22. Two-source power system with AG fault at remote end of the line, a) without any phase open in the parallel line and b) with Phase A open in the parallel line.

Table VIII lists the fault current phasors for the AG fault in Fig. 22 (a). As expected, the negative- and zero-sequence currents and the loop current with –7 degrees tilt have the same angle as the fault current angle, resulting in no errors in the corresponding reactance element reach. Refer to Section I for an explanation as to the effect of the polarizing current leading or lagging the fault current on the reactance element reach.

TABLE VIII
CURRENT PHASORS FOR THE AG FAULT IN FIG. 22 (A) (WITHOUT ANY PHASE OPEN IN THE PARALLEL LINE)

Phasor	Magnitude (A Primary)	Angle (Deg.)	Overreach (pu) in the Corresponding Reactance Element
$3 \bullet I_{2\_FLT}$	505	0	0
$3 \bullet I_{0\_FLT}$	505	0	0
I_{L_FLT} (with –7° tilt)	1415	0	0
I_{FLT}	4541	0	–

Table IX lists the current phasors for the AG fault in Fig. 22 (b). Note that Phase A of the parallel line is open during the fault. The negative- and zero-sequence currents and the loop current with –7 degrees tilt lead the total fault current phasor by 7, 5, and 3 degrees, respectively. The unbalanced condition (Phase A open in the parallel line) during the fault causes the polarizing currents to lead the fault current angle, resulting in overreach of the corresponding reactance elements. From Table IX, we can easily conclude that the negative-sequence, zero-sequence, and loop current polarized reactance elements need an additional tilt of –7, –5, and –3 degrees, respectively, to avoid overreach. However, this additional tilt may not guarantee addressing overreach concerns caused by other unbalanced operating conditions.

TABLE IX
CURRENT PHASORS FOR THE AG FAULT IN FIG. 22 (B) (WITH PHASE A OPEN IN THE PARALLEL LINE)

Phasor	Magnitude (A Primary)	Angle (Deg.)	Overrreach (pu) in the Corresponding Reactance Element
$3 \bullet I_{0\_UB}$	69	35	–
$3 \bullet I_{2\_UB}$	223	25	–
I_{L_UB}	821	26	–
$3 \bullet I_{2\_FLT}$	888	7	0.23
$3 \bullet I_{0\_FLT}$	615	5	0.17
I_{L_FLT} (with –7° tilt)	1793	3	0.10
I_{FLT}	4507	0	–

One of the ways to prevent overreach for faults during unbalanced operating conditions is to use incremental quantities in the polarizing currents. The incremental polarizing quantities are immune to the pre-fault conditions [21]. For the fault in Fig. 22 (b) and the phasors shown in Table IX, the incremental negative- and zero-sequence polarizing quantities are defined in (17) and (18).

$$\Delta\left(3 \bullet I_2\right) = 3 \bullet I_{2\_FLT} - 3 \bullet I_{2\_UB} \tag{17}$$

$$\Delta\left(3 \bullet I_0\right) = 3 \bullet I_{0\_FLT} - 3 \bullet I_{0\_UB} \tag{18}$$

The use of these incremental polarizing quantities ensures security of the corresponding reactance elements during unbalanced conditions. However, the main challenge with incremental quantities is their application over a short data window and their dependency on the pre-fault current (magnitude and angle) that may be prone to change. These limitations can be overcome by implementing a predefined polarizing quantity tilt angle determined by the maximum pre-fault unbalanced current magnitude and the minimum fault current magnitude for which the quadrilateral distance element is expected to pick up. Equations (19) and (20) define the negative- and zero-sequence current tilt angles that ensure security of the corresponding reactance elements for faults during unbalanced operating conditions.

$$\theta_{2\_UB} = -\tan^{-1}\left(\frac{\max\left|3 \bullet I_{2\_UB}\right|}{\min\left|3 \bullet I_{2\_FLT}\right|}\right) \tag{19}$$

$$\theta_{0\_UB} = -\tan^{-1}\left(\frac{\max\left|3 \bullet I_{0\_UB}\right|}{\min\left|3 \bullet I_{0\_FLT}\right|}\right) \tag{20}$$

Depending on the power system network configurations and unbalanced operating conditions, the tilt angles defined in (19) and (20) can be significant, i.e., –40 degrees or more. Tilting the reactance element characteristic by such a large angle can

drastically impact its dependability for typical faults (faults without unbalanced operating conditions). One way to increase security without sacrificing dependability is to set quadrilateral elements to allow a small amount of pre-fault unbalance by using a tilt angle smaller than the tilt angles defined by (19) or (20), e.g., –10 degrees. If the pre-fault unbalanced current magnitude exceeds the set limit, block the quadrilateral element while having the corresponding mho element running in parallel. This approach ensures the dependability of the Zone 1 distance elements. Some relays may include similar built-in logic in the distance elements to ensure Zone 1 security for faults during unbalanced operating conditions [22].

Fig. 23 shows the proposed logic of a simplified Zone 1 ground quadrilateral distance element for unbalanced operating conditions, assuming that the reactance element is polarized with zero-sequence current. Replace the I_0 terms with I_2 in Fig. 23, if the reactance element uses negative-sequence current polarization. The logic illustrated in Fig. 23, disables the Zone 1 quadrilateral element if the pre-fault unbalanced current magnitude ($|3 \bullet I_{0\_PRE\_FLT}|$) exceeds ($|3 \bullet I_0 \bullet \tan(\theta_{UB})|$). However, a small amount of pre-fault unbalanced current less than or equal to ($|3 \bullet I_0 \bullet \tan(\theta_{UB})|$) is securely compensated for by adding a clockwise tilt, (θ_{UB}) (e.g., –10 degrees), in the corresponding tilt angle setting. When ($|3 \bullet I_{0\_PRE\_FLT}|$) is greater than ($|3 \bullet I_0 \bullet \tan(\theta_{UB})|$), the Zone 1 quadrilateral distance element is disabled; therefore, the corresponding mho element is expected to run in parallel to maintain dependability of Zone 1 distance elements. Appendix C includes the relay instructions to implement the logic shown in Fig. 23.

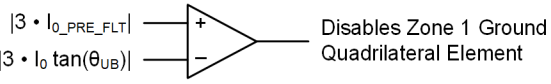

Fig. 23. Simplified Zone 1 ground quadrilateral distance element logic to prevent overreach for faults during unbalanced operating condition.

If the reactance elements use loop current polarization, follow the approach described in Section III.C with various unbalanced operating system contingencies to determine the required tilt to secure the reactance element for faults during unbalanced operating conditions. An incremental ground loop polarizing current is the summation of the incremental phase current and incremental ground current multiplied by the zero-sequence compensation factor (k_0). The incremental phase and ground currents follow the fault current angle; however, the angle of k_0 added to the incremental ground current may introduce significant difference between the angles of the incremental loop current and total fault current. Therefore, the use of incremental loop polarizing currents might work well for the phase loops; however, using them for the ground loops may result in overreach when the angle of the zero-sequence compensation factor (k_0) is positive.

Use the logic shown in Fig. 24 to disable the Zone 1 phase quadrilateral distance element, even for the slightest pre-fault unbalanced current given by ($|3 \bullet I_0| + |3 \bullet I_2| > 0.05 \bullet INOM$), while having the corresponding mho element running in parallel to maintain Zone 1 dependability. Comparing this logic to the logic shown in Fig. 23, we conclude that the logic in Fig. 24 does not need any additional tilt to compensate for unbalanced operating conditions; however, the lower fault resistance coverage of the mho element reduces the scheme dependability when the quadrilateral element is disabled.

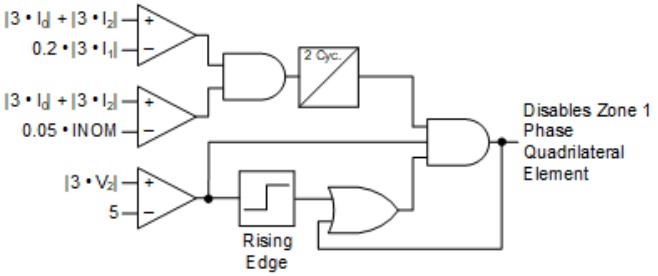

Fig. 24. Simplified Zone 1 phase quadrilateral distance element logic for small pre-fault unbalanced current.

The rising edge of ($|3 \bullet V_2| > 5$) in Fig. 24 indicates the inception of an unbalanced fault, while the two current comparators and the timer indicate a pre-fault unbalanced condition. If a previously balanced system experiences an unbalanced fault, the rising edge declaration expires before the two-cycle pickup timer times out, and the Zone 1 phase quadrilateral element is not disabled. With an unbalanced pre-fault condition, followed by an unbalanced fault, the pickup timer output is already high when the rising edge declaration occurs and the Zone 1 quadrilateral element is disabled. Appendix C includes the relay instructions to implement the logic shown in Fig. 24.

X. Determining the Best Tilt Angle for the Zone 1 Reactance Element

This section illustrates calculating the best tilt angle for the negative-sequence, zero-sequence, and loop current polarized Zone 1 reactance elements for the example system described in Fig. 7. Table X lists the tilt angle compensation needed for each of the factors affecting the security of the Zone 1 reactance elements. For simplicity, the Zone 1 quadrilateral distance elements are assumed to be configured with the proposed unbalanced operating condition logic described in Fig. 24. Therefore, no tilt angle compensation is considered for unbalanced operating conditions in Table X.

All of the compensating tilt angles shown in Table X for negative-sequence, zero-sequence, and loop polarizing quantities are calculated for line-end faults. For faults at the Zone 1 reach, the required clockwise tilt of the reactance characteristic is smaller than the total clockwise tilt of the reactance characteristic needed for faults at the end of the line. This angle difference is illustrated in Fig. 25, where $|\theta_{T\_Z1R}| < |\theta_{T\_Z1L}|$. In Fig. 25, Z_{1R} is the positive-sequence line impedance corresponding to the Zone 1 reach, θ_{Z1L} is the positive-sequence line impedance angle, θ_{T_Z1L} is the total tilt angle of the reactance characteristic for faults at the end of the line and including the outgoing load effect, θ_{T_Z1R} is the total tilt angle for faults at the Zone 1 reach, and R_{SET} is the user-defined right resistance blinder setting.

TABLE X
FACTORS AFFECTING THE SECURITY OF THE ZONE 1 REACTANCE ELEMENTS AND CORRESPONDING TILT ANGLE COMPENSATION FOR THE FIG. 7 EXAMPLE SYSTEM

Factors Affecting Zone 1 Reactance Element Security	Tilt Angle Compensation for Reactance Elements Polarized With		
	Negative-Sequence Current	Zero-Sequence Current	Loop Current
Network nonhomogeneity	–10° (θ_{2_NW})	–12° (θ_{0_NW})	(Tilt angle included in maximum outgoing load factor)
Maximum outgoing load (without unbalanced operating conditions)	NA	NA	–34° (θ_{L_LOAD})
VT and CT (steady state angle errors)	–7° ($\theta_{2\_VT\_CT}$)	–7° ($\theta_{0\_VT\_CT}$)	–7° ($\theta_{L\_VT\_CT}$)
Line charging current	0° (θ_{2_LCC})	0° (θ_{0_LCC})	–1° (θ_{L_LCC})
Untransposed line	–2° (θ_{2_UNTR})	–1° (θ_{0_UNTR})	0° (θ_{L_UNTR})
Unbalanced operating conditions*	0° (θ_{2_UB})	0° (θ_{2_UB})	0° (θ_{L_UB})
Total Tilt	**–19°**	**–20°**	**–42°**

* Zone 1 quadrilateral distance elements are assumed to be disabled for unbalanced operating conditions based on the logic described in Fig. 24. Therefore, no tilt angle compensation is needed for any of the polarizing quantities for unbalanced operating conditions.

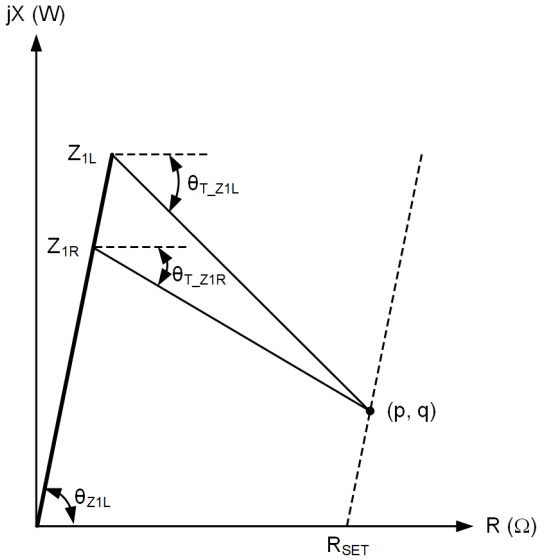

Fig. 25. Tilt angles for faults at the Zone 1 reach (θ_{T_Z1R}) and at the end of the line (θ_{T_Z1L}).

Use the corresponding Equations (21), (22), or (23) to determine the best tilt angles for the negative-sequence, zero-sequence, and loop current polarized Zone 1 reactance elements. Set the tilt angle setting meant for ground and phase reactance loops to the corresponding best tilt angle. In [9], set the TANG setting to the corresponding best tilt angle.

$$\theta_{2\_BEST} = \theta_{2\_T\_Z1R} - \theta_{L\_LOAD} + \theta_{2\_NW} \quad (21)$$

$$\theta_{0\_BEST} = \theta_{0\_T\_Z1R} - \theta_{L\_LOAD} + \theta_{0\_NW} \quad (22)$$

$$\theta_{L\_BEST} = \theta_{L\_T\_Z1R} \quad (23)$$

where:

$$\theta_{[k]\_T\_Z1R} = \tan^{-1}\left(\frac{q_{[k]} - \mathrm{Im}(Z_{1R})}{p_{[k]} - \mathrm{Re}(Z_{1R})}\right)$$

$$[k] = \{0, 2, L\}$$

$$p_{[k]} = \frac{\mathrm{Im}(Z_{1L}) - \tan\left(\theta_{[k]\_T\_Z1L}\right) \bullet \mathrm{Re}(Z_{1L}) + R_{SET} \bullet \tan(\theta_{Z1L})}{\tan(\theta_{Z1L}) - \tan\left(\theta_{[k]\_T\_Z1L}\right)}$$

$$q_{[k]} = \tan(\theta_{Z1L}) \bullet p_{[k]} - R_{SET} \bullet \tan(\theta_{Z1L})$$

$$\theta_{[k]\_T\_Z1L} = \theta_{L\_LOAD} + \theta_{[k]\_VT\_CT} + \theta_{[k]\_LCC} + \theta_{[k]\_UNTR} + \theta_{[k]\_UB}$$

$\theta_{[k]\_T\_Z1L}$ contains θ_{L_LOAD} which also includes network nonhomogeneity compensation for both negative-sequence and zero-sequence polarizing quantities. Therefore, $\theta_{[k]\_T\_Z1R}$ (derived from $\theta_{[k]\_T\_Z1L}$) requires further modifications in order to properly compensate the negative-sequence or zero-sequence polarizing quantities individually. Equations (21) and (22) add the corresponding θ_{2_NW} and θ_{0_NW} nonhomogeneity compensation angles and subtract θ_{L_LOAD} in both equations due to the insensitivity of negative-sequence and zero-sequence currents to load flow.

For the Fig. 7 example system, Fig. 26 shows the plots of the best tilt angles for the negative-sequence, zero-sequence, and loop current polarized Zone 1 reactance elements for different values of R_{SET} obtained from (21), (22), and (23), respectively.

As expected, the best tilt angles in Fig. 26 approach the corresponding total tilt angles of Table X as the value of R_{SET} increases. Fig. 26 illustrates that, as R_{SET} increases, the required clockwise tilt angle to keep the reactance element secure also increases. This observation is important because selecting the appropriate current polarized clockwise tilt angle from Fig. 26 affects the fault resistance coverage.

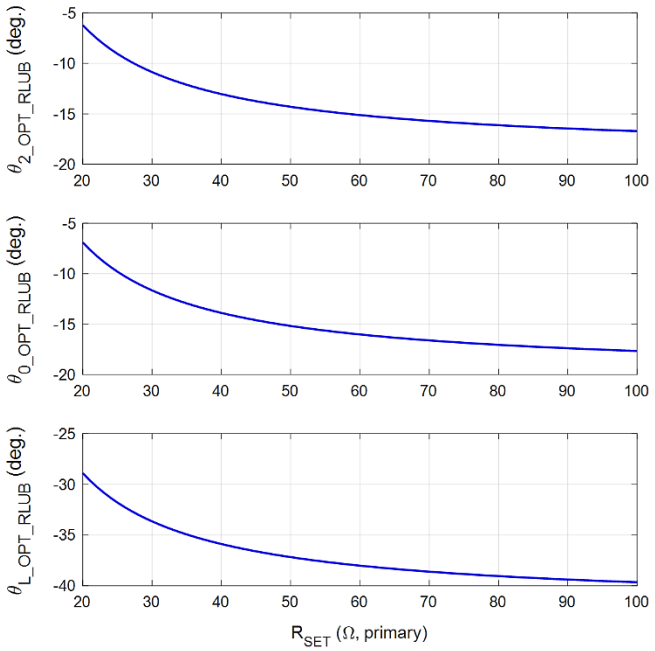

Fig. 26. Best tilt angles for negative-sequence, zero-sequence, and loop current polarized Zone 1 reactance elements for different values of R_{SET} for the Fig. 7 example system.

Fig. 27 illustrates the effect of the clockwise tilt of the reactance characteristic on the fault resistance coverage. A lower clockwise tilt of the reactance characteristic (A in Fig. 27) increases fault resistance coverage near the reactance reach; however, it decreases fault resistance coverage for the rest of the protected zone. This assessment is true because the right resistance blinder (R_{SET_A} in Fig. 27) has to be set lower for lower clockwise tilt angles. Whereas, a higher clockwise tilt of the reactance characteristic (in Fig. 27) may have reduced fault resistance coverage near the reach; however, it has high fault resistance coverage for the rest of the protected zone. This assessment is true because the right resistance blinder (R_{SET_B} in Fig. 27) can be set higher with higher clockwise tilt angles.

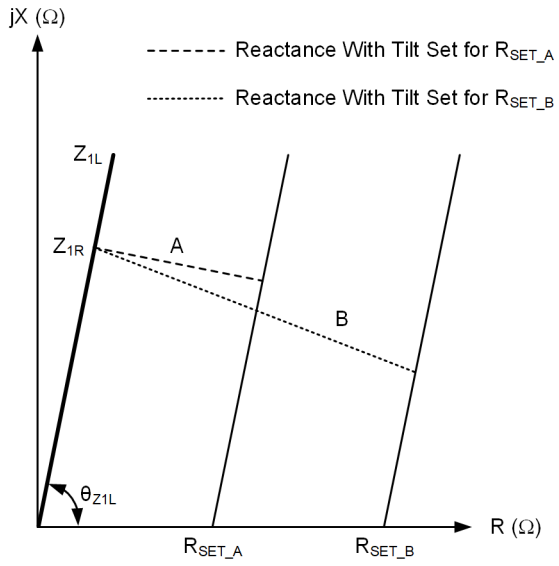

Fig. 27. Effect of the clockwise tilt of the reactance characteristic on the fault resistance coverage.

Knowledge of the effect of clockwise tilt of the reactance characteristic on the fault resistance coverage and maximum fault resistance that a given line may experience is useful in determining R_{SET} and tilt angle settings. Choose an appropriate R_{SET} and its corresponding clockwise tilt angle from the best tilt angle plots, such as the ones shown in Fig. 26, derived for that particular line. Using this R_{SET} with the corresponding clockwise tilt angle for the reactance element characteristic enhances the resistive coverage and ensures security of the Zone 1 reactance element.

XI. Conclusion

The reactance element defines the reach of the quadrilateral distance element. The combination of reactance element characteristic with adequate clockwise tilt and the right resistance blinder ensures security of the Zone 1 quadrilateral distance element for resistive faults. Factors like network nonhomogeneity, line loading, VT and CT steady-state angle errors, line charging currents, untransposed lines, zero-sequence mutual coupling, and unbalanced operating conditions may result in reactance element overreach for resistive faults. Typically, overreach of the Zone 1 reactance element for resistive line-end faults is compensated through clockwise tilt of the reactance characteristic. This paper describes how to set the tilt angle of the reactance characteristic to add security to Zone 1 of quadrilateral distance elements without sacrificing operating time for resistive faults and a given right resistance blinder setting.

This paper describes conditions and provides equations to determine an adequate negative- and zero-sequence network nonhomogenous correction angle. The conditions include faults at the Zone 1 reach and the end of the line with a weak source impedance behind the relay and the strongest source impedance beyond the remote bus.

Mutual coupling does affect the zero-sequence polarizing current angle; however, proper use of the equations provided in this paper compensates for that effect. Special considerations are described in this paper to determine nonhomogenous correction angles for lines with impedance angles less than 70 degrees.

Line loading does not affect negative- and zero-sequence current polarization. However, it has significant impact on loop current polarization, especially for outgoing loading conditions. This paper recommends simulating line-end faults with maximum outgoing power flow for all possible source impedances and different fault resistances to determine the loop current polarization tilt angle solely for outgoing loading conditions.

This paper provides an equation to calculate the error in the reactance element reach as a function of VT and CT steady-state angle errors. This equation shows that for given VT and CT angle errors, the reach error of the reactance element increases significantly as the fault resistance increases. This paper recommends simulating metallic line-end faults with heavy loading and the weakest source behind the relay to determine an adequate clockwise tilt angle required to compensate for VT and CT angle errors. This paper also shows

that the polarizing currents may have higher angle errors than the steady-state CT angle error in the faulted phase current. When CT saturation for line-end faults causes overreach, secure Zone 1 by appropriately reducing its reach.

The tilt angle setting needed to compensate for line charging current and line transpositions can be in the order of a couple of degrees. This paper defines an approach to determine this compensation.

Faults during unbalanced operating conditions are probably rare; however, they can significantly impact the security of the current polarized reactance element. This paper describes various approaches to compensate for unbalanced operating conditions. The simplest approach is to block Zone 1 quadrilateral elements for faults during unbalanced operating conditions, while having the corresponding mho element running in parallel.

Lastly, this paper provides an expression to determine the best tilt angle for a given right resistance blinder setting to enhance the fault resistance coverage and ensure security of the Zone 1 quadrilateral distance element.

XII. Appendix A

Deriving Expression for Negative-Sequence Nonhomogenous Network Correction Angle for Parallel Line Configuration

Fig. 28 shows a negative-sequence network for a fault at distance *m* from the local terminal in a parallel line configuration.

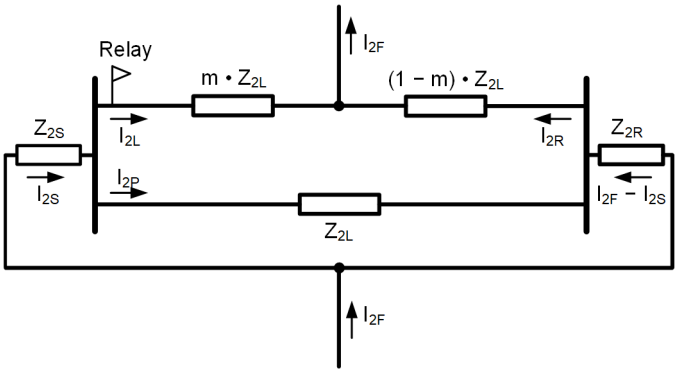

Fig. 28. Negative-sequence network for a fault at distance *m* from the relay in a parallel line configuration.

Equating negative-sequence voltage drops from the local bus to the remote bus through protected line and parallel line, we get:

$$I_{2P} \bullet Z_{2L} = m \bullet I_{2L} \bullet Z_{2L} - (1-m) \bullet I_{2R} \bullet Z_{2L} \tag{24}$$

Simplifying (24), we get:

$$I_{2P} = m \bullet I_{2L} - (1-m) \bullet I_{2R} \tag{25}$$

From Fig. 28,

$$I_{2R} = I_{2P} + I_{2F} - I_{2S} \tag{26}$$

Substituting (26) in (25), results in:

$$I_{2P} = I_{2L} - (1-m) \bullet I_{2F} \tag{27}$$

From Fig. 28,

$$I_{2S} = I_{2L} + I_{2P} \tag{28}$$

Substituting (27) in (28), we get:

$$I_{2S} = 2 \bullet I_{2L} - (1-m) \bullet I_{2F} \tag{29}$$

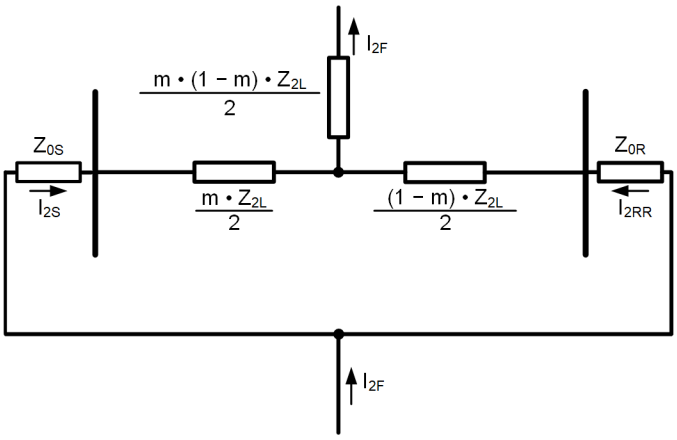

Fig. 29. Star-configuration impedances from the delta-configuration impedances of Fig. 28.

From Fig. 28,

$$I_{2S} = \frac{\frac{(1-m) \bullet Z_{2L}}{2} + Z_{2R}}{Z_{2S} + \frac{Z_{2L}}{2} + Z_{2R}} \bullet I_{2F} \tag{30}$$

Equating (29) and (30), and solving for I_{2L} / I_{2F}, results in:

$$\frac{I_{2L}}{I_{2F}} = \frac{(1-m) \bullet (Z_{2S} + Z_{2L} + Z_{2R}) + Z_{2R}}{2 \bullet \left(Z_{2S} + \frac{Z_{2L}}{2} + Z_{2R} \right)} \tag{31}$$

From(31),

$$\arg\left(\frac{I_{2F}}{I_{2L}}\right) = -\arg\left[\frac{(1-m) \bullet (Z_{2S} + Z_{2L} + Z_{2R}) + Z_{2R}}{2 \bullet \left(Z_{2s} + \frac{Z_{2L}}{2} + Z_{2R} \right)} \right] \tag{32}$$

Equation (32) represents the negative-sequence nonhomogenous network correction angle for a parallel line configuration having two lines, originating from and terminating on a common bus.

XIII. Appendix B

Deriving an Expression for Error in the Reactance Element Reach

Consider a fault at a distance *m* per unit from the relay, as shown in Fig. 30.

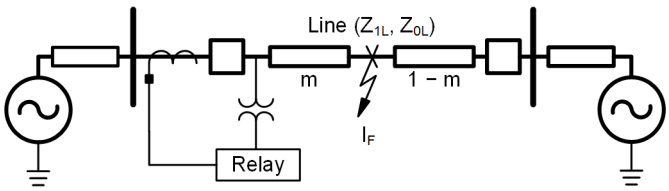

Fig. 30. Two-source power system with a fault at a distance *m* per unit from the relay.

The voltage V_L at the relay location can be expressed as:

$$V_L = m \bullet Z_{1L} \bullet I_L + I_F \bullet R_F \tag{33}$$

Multiplying both the sides of the previous equation by the conjugate of the fault current I_F and taking imaginary parts to solve for *m*, we get:

$$m = \frac{\mathrm{Im}\left[V_L \bullet I_F^*\right] - \mathrm{Im}\left[I_F \bullet R_F \bullet I_F^*\right]}{\mathrm{Im}\left[Z_L \bullet I_L \bullet I_F^*\right]} \tag{34}$$

We know, $\mathrm{Im}\left[I_F \bullet R_F \bullet I_F^*\right] = 0$,

$$\therefore m = \frac{\mathrm{Im}\left[V_L \bullet I_F^*\right]}{\mathrm{Im}\left[Z_{1L} \bullet I_L \bullet I_F^*\right]} \tag{35}$$

In polar form, the previous equation can be written as

$$m = \frac{|V_L| \bullet \sin\left(\theta_{V_L} - \theta_{I_F}\right)}{|Z_{1L} \bullet I_L| \bullet \sin\left(\theta_{Z_{1L}} + \theta_{I_L} + \theta_{I_F}\right)} \tag{36}$$

In (36), θ_{IF} is the fault current angle. Assume the polarizing current angle with appropriate tilt (θ_P) is same as the fault current angle. Substituting θ_{IF} by θ_P in (36), we get

$$m = \frac{|V_L| \bullet \sin\left(\theta_{V_L} - \theta_P\right)}{|Z_{1L} \bullet I_L| \bullet \sin\left(\theta_{Z_{1L}} + \theta_{I_L} - \theta_P\right)} \tag{37}$$

The primary and relay CTs introduce magnitude and angle errors in the loop and polarizing currents. Similarly, the primary and relay VTs introduce magnitude and angle errors in the faulted phase voltage. The line parameters may also be erroneous. Considering all these errors in (37), results in an error of the reactance reach δ_m as expressed in (38).

$$m + \delta m = \frac{|V_L + \delta V_L|}{|(Z_{1L} + \delta Z_{1L}) \bullet (I_L + \delta I_L)|} \bullet \frac{\sin\left(\theta_{V_L} + \delta\theta_{V_L} - \theta_P - \delta\theta_P\right)}{\sin\left(\theta_{Z_{1L}} + \delta\theta_{Z_{1L}} + \theta_{I_L} + \delta\theta_{I_L} - \theta_P - \delta\theta_P\right)} \tag{38}$$

Dividing equation (38) by (37), results in:

$$\frac{m + \delta m}{m} = \frac{|V_L + \delta V_L|}{|(Z_L + \delta Z_{1L}) \bullet (I_L + \delta I_L)|} \bullet \frac{|Z_{1L} \bullet I_L|}{|V_L|} \bullet \frac{\sin\left(\theta_{V_L} + \delta\theta_{V_L} - \theta_P - \delta\theta_P\right)}{\sin\left(\theta_{Z_{1L}} + \delta\theta_{Z_{1L}} + \theta_{I_L} + \delta\theta_{I_L} - \theta_P - \delta\theta_P\right)} \bullet \frac{\sin\left(\theta_{Z_{1L}} + \theta_{I_L} - \theta_P\right)}{\sin\left(\theta_{V_L} - \theta_P\right)} \tag{39}$$

Simplifying (39) with the following assumptions:

- The angle error ($\delta\theta_{IL} + \delta\theta_{Z1L} - \delta\theta_P$) is less than 20 degrees; therefore, $\cos(\delta\theta_{IL} + \delta\theta_{Z1L} - \delta\theta_P) \approx 1$, and $\sin(\delta\theta_{IL} + \delta\theta_{Z1L} - \delta\theta_P) \approx (\delta\theta_{IL} + \delta\theta_{Z1L} - \delta\theta_P)$.
- Similarly, the angle error ($\delta\theta_{VL} - \delta\theta_{IF}$) is less than 20 degrees; therefore, $\cos(\delta\theta_{VL} - \delta\theta_{IF}) \approx 1$, and $\sin(\delta\theta_{VL} - \delta\theta_{IF}) \approx (\delta\theta_{VL} - \delta\theta_{IF})$.

The result of these assumptions is shown in (40).

$$\frac{m + \delta m}{m} \approx \frac{|V_L + \delta V_L|}{|V_L|} \bullet \frac{|Z_{1L}|}{|Z_{1L} + \delta Z_{1L}|} \bullet \frac{|I_L|}{|I_L + \delta I_L|} \bullet \frac{1 + \cot\left(\theta_{V_L} - \theta_P\right) \bullet \left(\delta\theta_{V_L} - \delta\theta_P\right)}{1 + \cot\left(\theta_{I_L} + \theta_{Z_{1L}} - \theta_P\right) \bullet \left(\delta\theta_{I_L} + \delta\theta_{Z_{1L}} - \delta\theta_P\right)} \tag{40}$$

We assume that the loop current angle θ_{IL} follows the fault current angle θ_{IF}. However, even if there is significant difference between the two, the term $\cot(\theta_{IL} + \theta_{Z1L} - \theta_P) \bullet (\delta\theta_{IL} + \delta\theta_{Z1L} - \delta\theta_P)$ in the denominator of (40) shall be less than one; therefore, neglecting it, results in:

$$\frac{m + \delta m}{m} \approx \frac{|V_L + \delta V_L|}{|V_L|} \bullet \frac{|Z_{1L}|}{|Z_{1L} + \delta Z_{1L}|} \bullet \frac{|I_L|}{|I_L + \delta I_L|} \bullet \left[1 + \cot\left(\theta_{V_L} - \theta_P\right) \bullet \left(\delta\theta_{V_L} - \delta\theta_P\right)\right] \tag{41}$$

To get the amount of overreach for a fault at the end of the line, substitute $m = 1$ in (41) and substituting θ_P by θ_{IF} as assumed in (37).

$$\delta m \approx \left\{ \frac{|V_L + \delta V_L|}{|V_L|} \bullet \frac{|Z_{1L}|}{|Z_{1L} + \delta Z_{1L}|} \bullet \frac{|I_L|}{|I_L + \delta I_L|} \bullet \left[1 + \cot\left(\theta_{V_L} - \theta_{IF}\right) \bullet \left(\delta\theta_{V_L} - \delta\theta_P\right)\right] \right\} - 1 \tag{42}$$

Equation (42) provides an approximate expression for the error in the reactance reach. Negative values of δm indicate overreach, whereas positive values mean underreach.

Assuming negligible error in the magnitudes of the faulted phase voltage, line impedance, and loop current, the error in the reactance reach in (42) is solely because of VT and CT steady-state angle errors and is expressed as:

$$\delta m_{IT\_ANG} \approx \cot\left(\theta_{V_L} - \theta_{IF}\right) \bullet \left(\delta\theta_{V_L} - \delta\theta_P\right) \tag{43}$$

where:

$(\theta_V - \theta_P)$ is the angle difference between the faulted phase voltage at the relay location and the total fault current, (θ_P is assumed to be the total fault current angle, or else include that error in $\delta\theta_P$).

$\delta\theta_{VL}$ is the error in the faulted phase voltage angle because of the primary and relay VTs.

$\delta\theta_P$ is the error in the polarizing current angle because of the primary and relay CTs, or in other words, it is the angle difference between the relay calculated polarizing current and total fault current.

Note that (43) is an approximate expression and therefore may have numerical errors if the simplifying assumptions made in (39) are violated. However, (43) is still valuable for illustrating the effect of instrument transformer angle errors on reach estimation.

CT saturation results in reduced magnitude and a leading phase angle shift of the affected current phasor [18]. Assuming negligible error in the magnitude and angle of the faulted phase voltage and in the magnitude of line impedance, the error in the

reactance reach in (42) is solely because of CT saturation and is expressed as:

$$\delta m_{CT\_SAT} \approx \left\{ \frac{|I_L|}{|I_L + \delta I_L|} \bullet \left[1 - \cot\left(\theta_{V_L} - \theta_{IF}\right) \bullet \left(\delta\theta_P\right) \right] \right\} - 1 \tag{44}$$

where:

δI_L is the error in the loop current magnitude because of CT saturation.

$\delta\theta_P$ is the error in the polarizing current angle because of CT saturation, or in other words, is the angle difference between the relay calculated polarizing current and the total fault current.

Note (44) may not be accurate for severe CT saturation conditions because the angle error assumptions made when deriving (42) may get violated. However, the parameters (δI_L, θ_{VL}, θ_{IF}, and $\delta\theta_P$) in (44) affecting the error in the reactance reach because of CT saturation still stand true.

XIV. Appendix C

Relay Instructions to Implement the Logic Shown in Fig. 23 and Fig. 24

Note that PMV and PSV used in this section are IEEE 32-bit floating-point and Boolean variables, respectively.

1. Relay instructions for the logic described in Fig. 23 for Zone 1 quadrilateral ground distance element with zero-sequence current polarization for the reactance element.

PMV01 := 240.000000 # ENTER CTRW.
PSV01 := R_TRIG 3V2FIM > 5.000000 # INDICATES INCEPTION OF UNBALANCED FAULT.
PSV02 := 3V2FIM > 5.000000 # UNBALANCED FAULT.
PMV02 := LIGM * PSV01 / PMV01 + PMV02 * PSV02 # PRE-FAULT GROUND CURRENT MAGNITUDE.
PMV03 := LIGFIM * 0.176327 # TAN(10 DEG) = 0.176327. REMEMBER TO ADD ADDITIONAL -10 DEG. CLOCKWISE TILT IN THE TANGG SETTING FOR THIS LOGIC.
PSV03 := PMV03 > PMV02 AND PSV02 # USE PSV03 IN Z1XGTC.

2. Relay instructions for the logic described in Fig. 23 for Zone 1 quadrilateral ground distance element with negative-sequence current polarization for the reactance element.

PMV04 := 240.000000 # ENTER CTRW.
PSV04 := R_TRIG 3V2FIM > 5.000000 # INDICATES INCEPTION OF UNBALANCED FAULT.
PSV05 := 3V2FIM > 5.000000 # UNBALANCED FAULT.
PMV05 := L3I2M * PSV04 / PMV04 + PMV05 * PSV05 # PRE-FAULT NEGATIVE SEQ. CURRENT MAG.
PMV06 := L3I2FIM * 0.176327 # TAN(10 DEG) = 0.176327. REMEMBER TO ADD ADDITIONAL -10 DEG. CLOCKWISE TILT IN THE TANGG SETTING FOR THIS LOGIC.
PSV06 := PMV06 > PMV05 AND PSV05 # USE PSV06 IN Z1XGTC.

3. Relay instructions for the logic described in Fig. 23 for Zone 1 quadrilateral phase-distance element with negative-sequence current polarization for the reactance element.

PMV07 := 240.000000 # ENTER CTRW.
PSV07 := R_TRIG 3V2FIM > 5.000000 # INDICATES INCEPTION OF UNBALANCED FAULT.
PSV08 := 3V2FIM > 5.000000 # UNBALANCED FAULT.
PMV08 := L3I2M * PSV07 / PMV07 + PMV08 * PSV08 # PRE-FAULT NEGATIVE SEQ. CURRENT MAG.
PMV09 := L3I2FIM * 0.176327 # TAN(10 DEG) = 0.176327. REMEMBER TO ADD ADDITIONAL -10 DEG. CLOCKWISE TILT IN THE TANGP SETTING FOR THIS LOGIC.
PSV09 := PMV09 > PMV08 AND PSV07
PSV10 := PSV09 OR NOT 32QE # USE PSV10 IN Z1XPTC.

4. Relay instructions for the logic described in Fig. 24 for Zone 1 quadrilateral ground- and phase-distance element.

PMV10 := LIGFIM + L3I2FIM
PMV11 := 0.200000 * 3.000000 * LI1FIM
PMV12 := 0.050000 * 5.000000 # MULTIPLER 5 IS FOR 5A INOM RELAY. USE 1 for 1A INOM RELAY.
PSV11 := PMV10 > PMV11 AND PMV10 > PMV12
PCT01IN := PSV11 # INPUT TO TIMER PCT01
PCT01PU := 2.000000 # TWO POWER SYSTEM CYCLES PICKUP DELAY.
PCT01DO := 0.000000 # 0 DROP OUT DELAY.
PSV12 := R_TRIG 3V2FIM > 5.000000 # INDICATES INCEPTION OF UNBALANCED FAULT.
PSV13 := 3V2FIM > 5.000000 # UNBALANCED FAULT.
PSV14 := PCT01Q AND PSV12 OR PSV14 AND PSV13 # USE PSV14 IN Z1XGTC.
PSV15 := PSV14 OR NOT 32QE # USE PSV16 IN Z1XPTC.

XV. References

[1] A. R. van C. Warrington, *Protective Relays: Their Theory and Practice Volume One*, Chapman and Hall, Ltd., London, 1962.

[2] J. B. Roberts, A Guzmán, and E. O. Schweitzer, III, "Z = V/I Does Not Make a Distance Relay," proceedings of the 20th Annual Western Protective Relay Conference, Spokane, WA, October 1993.

[3] C. Henville and R. Chowdhury, "Coordination of Resistive Reach of Phase and Ground Distance Elements," proceedings of the 48th Annual Western Protective Relay Conference, Spokane, WA, October 2021.

[4] *GEI-98339E Directional Ground Distance Relay Instructions, Type GCXG51A11 & Up*, GE Power Management.

[5] E. O. Schweitzer, III, and J. B. Roberts, "Distance Relay Element Design," proceedings of the 19th Annual Western Protective Relay Conference, Spokane, WA, October 1992.

[6] W. Schossig, "Distance Protection From Protection Relays to Multifunctional," *Protection, Automation & Control World*, Vol. 04, Spring 2008, pp. 71–76.

[7] G. Ziegler, *Numerical Distance Protection: Principles and Applications, 2nd Edition*, Publicis Corporate Publishing, Erlangen, Germany, 2006.

[8] F. Calero, A. Guzmán, and G. Benmouyal, "Adaptive Phase and Ground Quadrilateral Distance Elements," proceedings of the 36th Annual Western Protective Relay Conference, Spokane, WA, October 2009.

[9] *SEL-421-4, -5 Protection, Automation, and Control System Instruction Manual*. Available: selinc.com.

[10] B. Kasztenny, "Settings Considerations for Distance Elements in Line Protection Applications," proceedings of the 74th Annual Conference for Protective Relay Engineers, College Station, TX, March 2021.

[11] F. Calero, "Mutual Impedance in Parallel Lines – Protective Relaying and Fault Location Considerations," proceedings of the 34th Annual Western Protective Relay Conference, Spokane, WA, October 2007.

[12] D. A. Tziouvaras, H. J. Altuve, and F. Calero, "Protecting Mutually Coupled Transmission Lines: Challenges and Solutions," proceedings of the 67th Annual Conference for Protective Relay Engineers, College Station, TX, March 2014.

[13] R. Jimerson, A. Hulen, R. Chowdhury, N. Karnik, and B. Matta, "Application Considerations for Protecting Three-Terminal Transmission Lines," proceedings of the 74th Annual Conference for Protective Relay Engineers, College Station, TX, March 2021.

[14] H. J. Altuve, J. B. Mooney, and G. E. Alexander, "Advances in Series-Compensated Line Protection," proceedings of the 35th Annual Western Protective Relay Conference, Spokane, WA, October 2008.

[15] J. Vargas, A. Guzmán, and J. Robles, "Underground/Submarine Cable Protection Using a Negative-Sequence Directional Comparison Scheme," proceedings of the 26th Annual Western Protective Relay Conference, Spokane, WA, October 1999.

[16] D. Tziouvaras, J. Roberts, G. Benmouyal, and D. Hou, "The Effect of Conventional Instrument Transformer Transients on Numerical Relay Elements," proceedings of the 28th Annual Western Protective Relay Conference, Spokane, WA, October 2001.

[17] E. O. Schweitzer, III, K. Behrendt, and T. Lee, "Digital Communications for Power System Protection: Security, Availability, and Speed," proceedings of the 25th Annual Western Protective Relay Conference, Spokane, WA, October 1998.

[18] J. Mooney, "Distance Element Performance Under Conditions of CT Saturation," proceedings of the 61st Annual Conference for Protective Relay Engineers, College Station, TX, April 2008.

[19] R. Chowdhury, D. Finney, N. Fischer, and D. Taylor, "Determining CT Requirements for Generator and Transformer Protective Relays," proceedings of the 46th Annual Western Protective Relay Conference, Spokane, WA, October 2019.

[20] K. Dase and N. Fischer, "Computationally Efficient Methods for Improved Double-Ended Transmission Line Fault Locating," proceedings of the 45th Annual Western Protective Relay Conference, Spokane, WA, October 2018.

[21] G. Benmouyal and J. Roberts, "Superimposed Quantities: Their True Nature and Application in Relays," proceedings of the 26th Annual Western Protective Relay Conference, Spokane, WA, October 1999.

[22] *SEL-T401L Ultra-High-Speed Line Relay Instruction Manual*. Available: selinc.com.

XVI. Biographies

Kanchanrao Dase received his bachelor of engineering degree in electrical engineering in 2009 from Sardar Patel College of Engineering, University of Mumbai, India. He received his master of science degree in electrical engineering from Michigan Technological University, Houghton, MI, in 2015. From 2009 to 2014, he was a manager at Reliance Infrastructure Limited with a substation engineering and commissioning profile. Currently, he is working with Schweitzer Engineering Laboratories, Inc. (SEL) as a lead power engineer. His research interests include power system protection, substation automation, and fault locating. He currently hold five patents in power system protection and fault locating.

Armando Guzmán (M '95, SM '01) received his BSEE with honors from Guadalajara Autonomous University (UAG), Mexico. He received a diploma in fiber-optics engineering from Monterrey Institute of Technology and Advanced Studies (ITESM), Mexico, and his Master of Science and PhD in electrical engineering and Master of Engineering in computer engineering from the University of Idaho, USA. He served as regional supervisor of the Protection Department in the Western Transmission Region of the Federal Electricity Commission (the electrical utility company of Mexico) in Guadalajara, Mexico for 13 years. He lectured at UAG and the University of Idaho in power system protection and power system stability. Since 1993, he has been with Schweitzer Engineering Laboratories, Inc. in Pullman, Washington, where he is a distinguished engineer. He holds numerous patents in power system protection, fault locating, and monitoring. He is a senior member of IEEE.

Steven Chase received his bachelor of science degree in electrical engineering from Arizona State University in 2008 and his master of science degree in electrical engineering in 2009. He worked for two years as a substation design intern at Salt River Project, an Arizona water and power utility. He joined Schweitzer Engineering Laboratories, Inc. (SEL) in 2010, where he works as a senior power engineer in the research and development division. He is currently a registered PE in the state of Washington.

Brian Smyth received a B.S.E.E. and M.S.E.E. from Montana Tech at the University of Montana in 2006 and 2008, respectively. He joined Montana Tech as a visiting professor in 2008 and taught classes in electrical circuits, electric machinery, instrumentation and controls, and power system analysis. He joined Schweitzer Engineering Laboratories, Inc. (SEL) in 2009 as an associate power engineer in the research and development division. Brian is currently a senior engineer in the transmission department and is the co-inventor of two patents. In addition to working for SEL, Brian joined Montana Tech in 2014 as an Affiliate Professor, where he teaches courses in power system protection. He received the Distinguished Alumni award from Montana Tech in 2016 and the IEEE Southwest Montana Chapter Engineer of the Year award in 2017. He is an active IEEE member and a registered professional engineer in the state of Washington.